Hemin availability induces coordinated DNA methylation and gene expression changes in *Porphyromonas gingivalis*

Ricardo Costeira[1¶], Joseph Aduse-Opoku[2¶], Jon J Vernon[3], Francisco Rodriguez-Algarra[4], Susan Joseph[2], Deirdre A Devine[3], Philip D Marsh[3], Vardhman Rakyan[4], Michael A Curtis[2*^], Jordana T Bell[1*^]

[1]Department of Twin Research and Genetic Epidemiology, King's College London, London SE1 7EH, UK
[2]Centre for Host-Microbiome Interactions, Faculty of Dentistry, Oral & Craniofacial Sciences, King's College London, London SE1 9RT, UK
[3]Division of Oral Biology, School of Dentistry, University of Leeds, Leeds LS2 9LU, UK
[4]The Blizard Institute, Barts and The London School of Medicine and Dentistry, Queen Mary University of London, London E1 2AT, UK

* Corresponding authors
Email addresses: jordana.bell@kcl.ac.uk, mike.curtis@kcl.ac.uk

¶ These authors contributed equally to this work
^ These authors also contributed equally to this work

Short title: DNA methylation and expression in *P. gingivalis*

Word count: 7464

Abstract

Periodontal disease is a common chronic inflammatory disease. *Porphyromonas gingivalis* is an important bacterium in the development of the disease and expresses a variety of virulence determinants. Hemin (iron [III] protopotphyrin IX), an essential nutrient of this organism, whose concentration increases with increasing inflammation, is a global regulator of virulence in *P. gingivalis*: high hemin levels increase expression of several virulence determinants. However, the mechanism through which hemin influences bacterial gene expression is poorly understood. Bacterial DNA methylation has the potential to fulfil this mechanistic role. Here, we characterised the methylome of *P. gingivalis*, and compared its variation to transcriptomic changes in response to changes in hemin concentration.

Gene expression and DNA methylation profiling of *P. gingivalis* W50 was performed, following continuous culture in chemostats with excess or limited hemin, using Illumina RNA-Seq and Nanopore DNA sequencing. DNA methylation quantification was carried out for Dam/Dcm motifs and all-context N6-methyladenine (6mA) and 5-methylcytosine (5mC) base pair modifications. Differential expression and methylation in response to excess hemin availability are presented after multiple testing correction (FDR 5%).

In excess hemin there were 161 over- and 268 under-expressed genes compared to limited hemin. Genes under-expressed in excess hemin were involved in iron recruitment (the hemophore HmuY) and transport (TonB-dependent receptors), and those over-expressed were involved in iron-sulphur cluster binding. Hemin-dependent differentially methylation was observed for the Dam 'GATC' motif and all-context 6mA and 5mC, with 36, 49 and 47 signals, respectively. Coordinated genome-wide differential expression and methylation effects were observed in 6 genes encoding a Ppx/GppA family phosphatase, a lactate utilization protein, a 4-alpha-glucanotransferase, two ABC transporter proteins, and a hypothetical protein HMPREF1322_RS00730. The findings indicate that altered genome methylation occurs in response to the availability of hemin and give insights into the molecular mechanisms of regulation of virulence in this bacterium.

Author Summary

DNA methylation has important roles in bacteria, including in the regulation of transcription. *Porphyromonas gingivalis,* an oral pathogen in periodontitis, exhibits well-established gene expression changes in response to hemin availability. However, the gene regulatory processes underlying these effects remain unknown. To this end, we profiled the novel *P. gingivalis* epigenome, and assessed epigenetic and transcriptome variation under limited and excess hemin conditions. As expected, multiple gene expression changes were detected in response to limited and excess hemin conditions that reflect conditions associated with health and disease, respectively. Notably, we also detected differential DNA methylation signatures for the Dam 'GATC' motif and both all-context N6-methyladenine (6mA) and 5-methylcytosine (5mC) in response to hemin availability. Joint analyses identified a subset of coordinated changes in gene expression, 6mA, and 5mC methylation that target genes involved in lactate utilization and ABC transporters. The results identify novel regulatory processes underlying the mechanism of hemin regulated gene expression in *P. gingivalis*, with phenotypic impacts on its virulence in periodontal disease.

63 # Introduction

64 Teeth are secured in the mouth through the periodontal ligament, which is attached to the
65 subgingival root surface and the alveolar bone. Periodontal disease is a common chronic
66 inflammatory disease of the periodontal tissues that is driven by bacteria in subgingival microbial
67 biofilms on the root surface. In periodontal disease the integrity of the attachment tissues becomes
68 compromised leading to bleeding, gingival recession, formation of deep periodontal pockets and
69 periodontal bone loss; ultimately culminating in tooth loss in a susceptible host. Periodontitis is a
70 global health issue affecting both developed and developing nations (1, 2). Furthermore,
71 periodontitis is also associated with a range of extra-oral inflammatory conditions, such as diabetes
72 and cardiovascular disease, rheumatoid arthritis, Alzheimer's disease and pregnancy complications
73 (3-5).

74 During the progression from health to periodontal disease, the oral microbiota undergoes a major
75 transition wherein the microbial community increases in total bacterial diversity, accompanied by a
76 bloom in disease-associated bacteria which start to dominate the community, while being otherwise
77 present in low numbers in healthy microbiota (6, 7). *Porphyromonas gingivalis*, a black-pigmenting
78 anaerobic rod bacterium, is well established as one of the organisms which is positively associated
79 with this shift to a dysbiotic microbiota in disease. Indeed, *P. gingivalis* has been shown to act as a
80 trigger for the conversion of the subgingival microbiota to a more diverse and more pathogenic
81 community in animal models of disease (6, 7). This keystone pathogen behaviour has been
82 attributed to the expression of a variety of extracellular virulence determinants including those
83 trafficked through a Type IX secretion system (T9SS) and through the production of large numbers of
84 outer membrane vesicles, which are collectively able to destabilise the host-microbe homeostasis at
85 this mucosal surface (8, 9).

86 Hemin, iron (III) protoporphyrin IX chloride, is a major source of iron for a variety of organisms,
87 including *P. gingivalis* where it is an essential cofactor for growth. *P. gingivalis* has a dedicated
88 transport system to ensure an efficient accumulation of hemin on the surface for iron utilisation.
89 Subsequent conversion of hemin to μ-oxo bis-haem, and its complexation with iron III, leads to black
90 pigmentation of the bacterial cells, a prominent characteristic of *P. gingivalis* on solid media
91 containing blood (10). *P. gingivalis*, HmuY and HusA are dedicated, surface-exposed hemophore-like
92 proteins that scavenge and bind hemin, free or released from heme containing proteins by gingipain
93 proteases. The complexes deliver the bound heme to outer-membrane receptors for internalization
94 (HmuR or HusB) and heme is then imported through a dedicated TonB-dependent transport
95 machinery (11).

96 The concentration of environmental hemin acts as a regulator of virulence in this bacterium: cells
97 cultured in high concentrations of hemin - comparable to the situation in a diseased periodontium
98 with elevated bleeding - upregulate the expression of a wide variety of virulence determinants,
99 including a range of hydrolytic enzymes such as the gingipain cysteine proteases, and other protein
100 products many of unknown function (12, 13). High-hemin grown cells are significantly more
101 pathogenic in animal models of tissue destruction compared to cells grown under hemin limitation
102 (8, 14-16). Hence, the availability of hemin in the growth media is critical to the full expression of
103 virulence of *P. gingivalis* and hemin may be regarded as a global regulator of transcription in this
104 bacterium. Although previous studies have characterised the impact of hemin availability on gene
105 expression and virulence in *P. gingivalis*, the regulatory processes underlying these functional
106 changes are not well understood. However, the P. *gingivalis* ATCC33277– genome encodes seven
107 two-component signal transduction system (TCS) pairs of a response regulator and a histidine kinase

108 traditionally involved in gene regulation in other organisms (17). Recently it has been reported that
109 one of these TCS, PorX/PorY, responds to environmental hemin and through the co-ordinated action
110 of PorX and SigP regulates transcription of the T9SS and hemin accumulation; mutants defective in
111 either *porX* or *porY* are attenuated in a mouse model of virulence (18, 19). However, given the
112 magnitude of changes in response to the concentration of hemin, there may be other mechanisms
113 of hemin regulated gene expression in *P. gingivalis*.

114 Like eukaryotic genomes, bacterial genomes are subject to epigenetic modifications, specifically DNA
115 methylation, which has multiple roles in bacteria including the regulation of transcription. Bacterial
116 DNA methylation includes modifications N6-methyladenine (6mA), 5-methylcytosine (5mC), and N4-
117 methylcytosine (4mC), of which 6mA is most prevalent in prokaryotes. Recent development in single
118 molecule sequencing technologies, for example Nanopore sequencing, allow for the detection of
119 these multiple DNA methylation base modifications. Using this approach, bacterial DNA methylation
120 signatures have recently been shown to impact gene expression profiles and genome stability (20,
121 21).

122 In this study, we investigated the impact of hemin availability on the *P. gingivalis* epigenome and
123 transcriptome. *P. gingivalis* W50 was grown in controlled conditions, in continuous culture at a
124 constant pH and identical growth rates, under either limited hemin or excess hemin conditions.
125 Subsequently, DNA sequencing using Nanopore and RNA sequencing using Illumina were carried out,
126 to profile the *P. gingivalis* DNA methylome and transcriptome under each condition. Hemin-
127 dependent differentially modified signatures were identified for gene expression, as well as for 6mA
128 and 5mC DNA methylation profiles both in Dam/Dcm motifs and genome-wide. Comparison of the
129 signals highlighted a cluster of coordinated changes in 6 genes, including in genes related to lactate
130 utilisation and in ABC transporters.

131

132 Results

133 Gene expression and DNA methylation profiling of *P. gingivalis* W50 was performed after culturing in
134 chemostat runs with excess (5 mg L^{-1}) or limited hemin (0.2 mg L^{-1}). Biological replicates were
135 collected every 48-hours after achieving steady state, with three biological replicates per
136 experimental condition profiled using Illumina RNA-Seq and Nanopore DNA sequencing technologies
137 (Fig 1).

138 Continuous chemostat environment

139 Steady state was achieved by days 3 and 4 for excess and limited hemin (Fig 2), respectively. Colony
140 counts of *P. gingivalis* W50 were consistently higher in excess hemin culture versus limitation,
141 elevated by an average of 1.52×10^9 (range $3.44 \times 10^8 – 3.07 \times 10^9$) colony forming units per ml (CFU
142 mL^{-1}). OD_{600} ranged between 1.67–1.72 (mean 1.69) and 0.357–0.376 (mean 0.367), for excess and
143 limited hemin, respectively. The pH was automatically controlled at pH 7.0 ± 0.1 whilst temperature
144 remained between 36.7 and 37.1°C for both conditions. Bacteria were grown at an identical and
145 constant growth rate of 6.9h mean generation time under both conditions (16).

146 Gene expression changes

147 RNA-seq data for the six samples was processed using ProkSeq (22) and DESeq2 (23) to assess gene
148 expression changes observed after culturing *P. gingivalis* W50 in excess (treatment) and limited
149 (control) hemin conditions. These results were mapped to the *P. gingivalis* W50 genome (RefSeq
150 assembly accession no. GCF_000271945.1). Out of 1,192 total genes analysed, those with an

151 expression LFC > 1.5 or LFC < −1.5 were considered differentially expressed after multiple testing
152 correction (FDR = 5%).

153 Altogether, 161 and 268 differentially expressed genes (DEGs) were respectively over- and under-
154 expressed in excess hemin across the *P. gingivalis* genome (Fig 3). The 161 DEGs over-expressed in
155 excess hemin included genes encoding homologous proteins of the rubrerythrin family
156 (HMPREF1322_RS04040), 4Fe-4S cluster domain-contain containing proteins
157 (HMPREF1322_RS09700, HMPREF1322_RS04860, HMPREF1322_RS04425), a thiamine phosphate
158 synthase (HMPREF1322_RS02110), electron transport complex subunits (HMPREF1322_RS04875,
159 HMPREF1322_RS04865, HMPREF1322_RS01760, HMPREF1322_RS04880, HMPREF1322_RS04870,
160 HMPREF1322_RS04885, HMPREF1322_RS01765), SDR family/ferredoxin oxidoreductases
161 (HMPREF1322_RS07305, HMPREF1322_RS04445, HMPREF1322_RS04440, HMPREF1322_RS00310)
162 and several dehydrogenases (*e.g.* HMPREF1322_RS07315, HMPREF1322_RS04430 and
163 HMPREF1322_RS06505) (Table 1; S1 Table). Methyltransferases targeting tRNA and 16S rRNA
164 molecules were also over-expressed in excess hemin (HMPREF1322_RS00530,
165 HMPREF1322_RS05610, HMPREF1322_RS04605). Most of these genes encode proteins that contain
166 iron as part of their tertiary structure. Three operonic genes, originally labelled as encoding TapA,
167 TapB and TapC (24), HMPREF1322_RS02140, HMPREF1322_RS02145, HMPREF1322_RS02150,
168 respectively, were also over-expressed. TapA, TapB and TapC contribute to virulence in a mouse
169 model as single isogenic mutants are attenuated. Both TapA and TapC exhibit the C-terminal domain
170 signature typical of the T9SS and are therefore cargo proteins as are the proteases
171 HMPREF1322_RS06795 (PrtT) and Lys-gingipain (Kgp).

172 The 268 DEGs under-expressed in excess hemin included genes *hmuY* (hemin-binding),
173 HMPREF1322_RS06790 (hemin transport), and those encoding homologues of at least 35
174 transposases (*e.g.* HMPREF1322_RS07370, HMPREF1322_RS07285, HMPREF1322_RS10850) (Table
175 2; S2 Table). Other genes under-expressed in excess hemin conditions included genes coding
176 several transporter proteins, with at least eight genes coding ABC transporter proteins (*e.g.*
177 HMPREF1322_RS00745, HMPREF1322_RS00115, HMPREF1322_RS08925). Two genes coding for
178 class I SAM-dependent methyltransferases (HMPREF1322_RS07630, HMPREF1322_RS07185) and
179 one gene coding for an isoprenylcysteine carboxylmethyltransferase family protein
180 (HMPREF1322_RS07190) were under-expressed in excess hemin conditions. The gene encoding the
181 largest protein component of the T9SS, Sov (SprA), and also genes encoding OmpH, PorN (GldN) and
182 PorX along with five cargo proteins, are under-expressed in excess hemin (S2 Table).

183 Different types of genes involved in virulence were identified in both the under- and over-expressed
184 DEG subsets. For example, these included different types of N-acetylmuramoyl-L-alanine amidase
185 genes, T9SS type A sorting domain-containing protein genes and MATE family efflux transporter
186 genes, and tetratricopeptide repeat protein genes were identified (S1 and S2 Tables).

187

188 We explored molecular functions shared across the DEGs, although a proportion of genes were not
189 well characterised. Sixty-seven under-expressed (25% of total) and 19 over-expressed (12%) genes
190 identified during growth in excess hemin encoded hypothetical proteins. Additionally, only 16 (6%)
191 of under-expressed genes and 49 (30%) of over-expressed genes identified had well-characterised
192 annotations in RefSeq. A GO term enrichment analysis was carried out using ShinyGO and gene
193 symbols that matched genes in the reference strain *P. gingivalis* W83 (25), with altogether 8 (out of
194 16 well-characterised) under-expressed and 40 (out of 49 well-characterised) over-expressed genes.

195 Forty-two and 43 GO molecular functions were respectively enriched in genes under- and over-
196 expressed in excess hemin conditions. In both cases, molecular functions identified were mostly
197 related to binding activities such as cyclic compound binding, heterocyclic compound binding and
198 ion binding (Fig 4; S3 and S4 Tables). In excess hemin, functions related to Fe-S cluster binding,
199 4Fe-4S cluster binding and metal cluster binding, and several different catalytic activities, including
200 GTPase, metallo-endopeptidase, active transmembrane transporter and diphosphotransferase
201 activities were also identified (Fig 4; S4 Table).

202

203 Two sensitivity analyses were carried out for the genome-wide DESeq2 DEG results presented here.
204 A first sensitivity analysis was performed using edgeR, which normalizes expression data differently
205 to DESeq2, and consistently identified the majority of DEGs identified with DESeq2 (S1 Fig).
206 Specifically, edgeR identified 166 genes as over-expressed and 266 genes as under-expressed with
207 excess hemin, of which 161 and 265 were previously identified with DESeq2. In a second general
208 sensitivity analysis, a principal component analysis (PCA) of the genome-wide RNA-seq levels also
209 confirmed overall global differences in gene expression levels between the culturing conditions (S2
210 Fig).

211

212 DNA methylation changes

213 Nanopore sequencing data were generated for the same six biological samples analysed with
214 Illumina RNA sequencing. Dam and Dcm-dependent methylation was characterised using the Guppy
215 basecaller. A total of 12,066 'GATC' (Dam) and 819 'CCWGG' (Dcm) motifs with minimum 10×
216 coverage across samples were considered. Motif-independent methylation levels for 6mA and 5mC
217 were characterised using Tombo with 'all-context' models, considering >2M positions with a
218 minimum 10× coverage. PCA of the genome-wide DNA methylation levels pointed to both global
219 6mA and 5mC differences in *P. gingivalis* according to hemin culture conditions (S3-A Fig) and
220 mirrored the PCA pattern observed for gene expression (S1 Fig). Similar results were observed
221 when considering signals with at least 100× coverage (S3-B Fig), and Dam-dependent adenine
222 methylation alone (S4-A and S4-B Figs, top panels). Differential methylation analyses with
223 respect to hemin levels were then carried out, considering signals where at least 5% mean
224 methylation difference between the experimental conditions was observed after multiple testing
225 correction (FDR 5%).

226 Dam/Dcm DNA methylation

227 DNA methylation signals were analysed at 79 'GATC' motifs in the genome of *P. gingivalis* W50,
228 which had at least 5% mean methylation differences between hemin conditions. Of these, 36 motifs
229 showed statistically significant differential methylation signals across hemin conditions (S5 Table).
230 Differentially methylated 'GATC' motifs ('GATC'-DMMs) were located in altogether 32 genes,
231 including a zinc-dependent metalloprotease (HMPREF1322_RS05790), a thioredoxin-disulfide
232 reductase (HMPREF1322_RS01475) and a 4-alpha-glucanotransferase (HMPREF1322_RS03650). If
233 genes up to ±1 kb away from the 'GATC' motifs were considered, 85 genes were candidates for
234 possible Dam-like regulation. Sensitivity analysis at 100× coverage (66 motifs) identified 36
235 differentially methylated motifs as well, of which 34 were present in the main analysis (S6 Table).

236 No minimum 5% mean methylation difference was observed at each Dcm-associated 'CCWGG'
237 motif, in line with previous observation for no overall differences in the Dcm-based PCA analysis (S4-

238 A and S4-B Figs, bottom panels). This suggests either the absence of enzymes targeting
239 'CCWGG' motifs in *P. gingivalis* W50 or a minimal role of a Dcm-like response to hemin availability.

240 All-context 6mA/5mC DNA methylation

241 The proportion of differential methylation at each genomic position was analysed for altogether
242 139,794 adenines and 87,398 cytosines with at least 5% mean difference in DNA methylation levels
243 between conditions.

244 Forty-nine differentially methylated adenine sites (DMAs) were identified between experimental
245 conditions across the *P. gingivalis* W50 genome (Fig 5). A cluster of 15 DMAs was observed in a
246 genomic region (NZ_AJZS01000011.1 ≈ 12 – 20 kb) containing the (Fe-S)-binding protein
247 HMPREF1322_RS00720, lactate utilization protein HMPREF1322_RS00725, hypothetical protein
248 HMPREF1322_RS00730, PaaI family thioesterase HMPREF1322_RS00735 and ABC transporter ATP-
249 binding protein HMPREF1322_RS00740 (Fig 5 top panel, purple; Fig 6). In annotating DMAs to
250 genes, if genes up to ±1 kb away from the DMA on both strands were considered, all DMAs are
251 annotated to at least one gene for a total of 75 genes altogether. Furthermore, 25 DMAs were
252 annotated to genes on the same strand, including seven DMAs encoding a lactate utilization protein
253 (HMPREF1322_RS00725), five in a hypothetical protein (HMPREF1322_RS00730), and two each in a
254 4-alpha-glucanotransferase (HMPREF1322_RS03650) and a Ppx/GppA family phosphatase
255 (HMPREF1322_RS06180) (Table 3). Four DMAs were located within 1 kb of a gene encoding a (Fe-
256 S)-binding protein (HMPREF1322_RS00720). In a sensitivity analysis considering only adenines with
257 at least 100× coverage (85,090 adenines), 20 DMAs were identified at FDR = 5% (S7 Table) and all
258 20 were also identified in the results of the main analysis.

259 Forty-seven differentially methylated cytosines (DMCs) were identified between experimental
260 conditions across the *P. gingivalis* W50 genome (Fig 5). Two clusters of 15 and 12 DMCs emerged -
261 the first was the same as the DMA cluster region (NZ_AJZS01000011.1, ≈ 12 – 20 kb), and the second
262 was in a genomic region (NZ_AJZS01000050.1, ≈ 0 – 3.5 kb) containing the DUF2436 domain-
263 containing protein HMPREF1322_RS04325 and nucleoside permease HMPREF1322_RS04330 (Fig. 5
264 bottom panel, purple and green; Fig 6). Thirty-five DMCs were located in 16 genes including in
265 genes identified in the DMA analyses above. Specifically, four DMCs were located in genes encoding
266 the (Fe-S)-binding protein HMPREF1322_RS00720, two in the lactate utilization protein
267 HMPREF1322_RS00725, and two in the hypothetical protein HMPREF1322_RS00730 reported above
268 for 6mA. Single DMCs were also identified in the 4-alpha-glucanotransferase HMPREF1322_RS03650
269 and Ppx/GppA family phosphatase HMPREF1322_RS06180 genes (Table 4). Overall, if genes up to
270 ±1 kb away on both strands were considered, 31 genes harboured DMCs, of which 10 also harboured
271 DMAs. Other genes annotated to the DMCs identified included those encoding transporter proteins
272 such as an iron ABC transporter permease (HMPREF1322_RS01240) and others
273 (HMPREF1322_RS01245; HMPREF1322_RS06460). In sensitivity analysis considering only cytosines
274 with at least 100× coverage (46,930 cytosines), 47 DMCs were also identified, of which 27 were also
275 in the main analysis results (S8 Table).

276 We explored evidence for putative DNA sequence motifs at the identified all-context DMAs and
277 DMCs. First, we observed that the DMAs identified in this all-context analysis (Table 3) did not
278 overlap with our 'GATC'-DMM results (S5 Table). We observed, however, that the 4-alpha-
279 glucanotransferase HMPREF1322_RS03650 and the DUF3298 domain-containing protein
280 HMPREF1322_RS07770 contained respectively two and one DMAs within 500 bp of a differentially
281 methylated 'GATC' motif. Overall, DMAs and 'GATC'-DMMs shared 13 genes annotated within 1 kb
282 of their location (out of 75 and 85 genes respectively identified for DMAs and 'GATC'-DMMs) (S5

283 Table). Second, we searched for over-representation of up to 15-nucleotide long sequences
284 surrounding all DMAs and DMCs. Although the analyses identified putative sequences of length 10-
285 11 nucleotides, the results did not reach statistical significance (MEME E-value > 0.05; S5 Fig).

286

287 Genes with coordinated differential DNA methylation and expression changes

288 We assessed whether the observed DEGs also exhibited DNA methylation changes for 6mA and 5mC.
289 We first compared DEGs to DMAs and DMCs each (Fig 7), and then explored further genomic
290 regions that contained DEGs, DMAs, and DMCs (Fig 7).

291 Overall, 23 DEGs also harboured DMAs (Table 5; Table 6). Of these, 8 genes were over-expressed
292 in excess hemin including the SDR family oxidoreductase HMPREF1322_RS07305 (*P. gingivalis* W83:
293 PG2069) and the Ppx/GppA family phosphatase HMPREF1322_RS06180 (W83: PG1739) genes
294 (Table 5). In all 8 cases the DMA was on the same strand as the gene, located either in or upstream
295 of the gene (Table 5), with hypermethylation in excess hemin for most cases. The 15 DEGs with
296 DMAs under-expressed in excess hemin included the hypothetical protein HMPREF1322_RS00730
297 (W83: PG1173) in the lactate utilization cluster, the lactate utilization protein
298 HMPREF1322_RS00725 (W83: PG1172), the 4-alpha-glucanotransferase HMPREF1322_RS03650
299 (W83: PG0767) and ABC transporter protein gene cluster HMPREF1322_RS00745 (W83: PG1176)
300 and HMPREF1322_RS00740 (W83: PG1175) (Table 6). Seven of the 15 genes had DMAs located
301 upstream of the gene and six of these showed increased 6mA accompanied by decreased gene
302 expression, indicating a potential regulatory effect of 6mA in dampening the expression of *P.*
303 *gingivalis* genes according to hemin availability in the bacterium's microenvironment. Most DMAs
304 annotated to under-expressed genes had higher adenine methylation in excess hemin (84%)
305 regardless of their location with respect to gene structure. In comparison to all-context DMAs, the
306 'GATC'-DMMs were annotated to 14 DEGs (6 and 8 DEGs respectively over and under-expressed; S9
307 and S10 Tables). DEGs associated with 'GATC'-DMMs included among others the 4-alpha-
308 glucanotransferase HMPREF1322_RS03650 (W83: PG0767) mentioned immediately above.
309 However, only four genes had 'GATC'-DMMs upstream their start site, and another only two genes
310 showed greater methylation associated with lower expression overall. This suggests very limited
311 potential for a role of GATC methylation in the regulation of gene expression in *P. gingivalis* W50 in
312 response to hemin availability.

313 One over-expressed and 11 under-expressed genes also had DMCs within 1 kb of the gene (Tables
314 7 and 8). Two of the 11 under-expressed genes had DMCs upstream of the gene (Table 8) with
315 increased methylation levels observed for all 11 genes. Moreover, 95% of DMCs annotated to under-
316 expressed genes had increased cytosine methylation in excess hemin regardless of their location in
317 relation to the gene. This is consistent with results from 6mA, although knowledge of gene
318 regulation by 5mC methylation in bacteria remains limited.

319 Six DEGs had both DMAs and DMCs in their gene body or within ±1kb of the gene (Fig 7), and a
320 subset of these DEGs clustered in a genomic region that includes the lactate utilization gene cluster
321 (Fig 6). The 6 DEGs include the Ppx/GppA family phosphatase HMPREF1322_RS06180 (W83:
322 PG1739), over-expressed in excess hemin, and the hypothetical protein HMPREF1322_RS00730
323 (W83: PG1173), lactate utilization protein HMPREF1322_RS00725 (W83: PG1172), 4-alpha-
324 glucanotransferase HMPREF1322_RS03650 (W83: PG0767), ABC transporter protein
325 HMPREF1322_RS00745 (W83: PG1176), and HMPREF1322_RS00740 (W83: PG1175), which were
326 under-expressed in excess hemin (Table 9). We assessed whether genome-wide DEGs were

327 enriched for DMAs and DMCs, but did not observe a significant enrichment overall (OR = 0.77 (95%
328 CI: 0.45, 1.31), P-value = 0.38 and OR = 1.13 (95% CI: 0.49, 2.47), P-value = 0.85, respectively).
329 However, we observed strong evidence for overall differences in upstream or gene body DNA
330 methylation levels at specific DEGs overlapping DMAs and DMCs (S6 and S7 Fig).

331 For all DEGs that also harboured DMAs or DMCs, we analysed the overall levels of adenine (S6 Fig)
332 and cytosine (S7 Fig) methylation upstream (−100 bp), downstream (+100 bp) and in the gene body.
333 Differential adenine and cytosine methylation were observed across all regions analysed for the
334 lactate utilization protein HMPREF1322_RS00725 (W83: PG1172) (upstream; gene body;
335 downstream; Table 9; Fig 6). Differential adenine and cytosine methylation were also observed in
336 the gene body of the ABC transporters HMPREF1322_RS00740 (W83: PG1175) and
337 HMPREF1322_RS00745 (W83: PG1176), and hypothetical protein HMPREF1322_RS00730 (W83:
338 PG1173) (S6 and S7 Figs). These ABC transporter proteins are located directly downstream of a
339 lactate utilization gene cluster, which includes the lactate utilization protein and hypothetical
340 protein, possibly highlighting a key region of the *P. gingivalis* genome regulated by DNA methylation
341 (Fig 6). Overall changes in adenine and/or cytosine methylation were also for example observed in
342 the body of the 4−alpha−glucanotransferase HMPREF1322_RS03650 (W83: PG0767) gene, and
343 upstream the ABC transporter HMPREF1322_RS00740 (W83: PG1175) (S6 and S7 Figs).

344

345 Discussion

346 We identified a significant impact of hemin availability in the growth medium on the *P. gingivalis*
347 epigenome and transcriptome. Growth of *P. gingivalis* is restricted in the healthy gingival crevice due
348 to a tight restriction by the host on hemin availability. However, during increasing inflammation in
349 periodontal disease, the availability of heme-containing molecules is substantially increased. Hemin-
350 dependent differentially modified signatures were identified for gene expression, as well as for 6mA
351 and 5mC methylation profiles. Comparison of the signals highlighted a cluster of coordinated changes
352 in genes related to lactate utilisation and in ABC transporters. The findings identify putative bacterial
353 DNA methylation signatures that may play a regulatory role in the expression of genes, in response to
354 hemin availability.

355 Many of the genes that were over-expressed in excess hemin encoded proteins that contain iron as
356 part of their tertiary structures or iron binding domains in the polyprotein. Furthermore, Lys-
357 gingipain (Kgp; S1 Table) was also over-expressed, and it is involved in iron acquisition and is
358 essential for black pigment (μ-oxo bishaem) formation from hemin and its absence attenuates
359 virulence (15). Members of the ABC transport complex (Fig 6B and Table 6), forming a classical
360 operon, may potentially represent a novel hemin or alternative solute acquisition system that may
361 influence the cellular phenotype. The enhanced expression of thiamine phosphate synthase is not
362 only limited to this gene (S1 Table) of the pathway; the contig also encodes ThiH, ThiG, ThiC, ThiS
363 and a hypothetical protein, all arranged in an apparent operon. Thus, the biosynthesis of the energy
364 co-factor thiamine, vitamin B1, may constitute an important aspect of *P. gingivalis* metabolism.
365 Rubrerythin offers protection of the anaerobe, *P. gingivalis*, against the toxicity of molecular oxygen
366 and hydrogen peroxide; an isogenic mutant is labile under these conditions (26). In addition, there
367 appears to be a preference for succinate/fumarate and α-ketoglutarate utilisation (S1 Table).

368 Many genes under-expressed in excess hemin were involved in hemin binding or transport. Some
369 genes also encoded for DNA transfer functions such as TraC, TraE, TraF and TraJ. Interestingly, the
370 gene encoding the largest protein component of the type IX secretion system (T9SS), Sov (SprA), and

371 also genes encoding OmpH, PorN (GldN) and PorX along with five cargo proteins, are under-
372 expressed in excess hemin (S2 Table). The complex transports over 30 cargo proteins, including
373 known virulence factors, with a C-terminal domain (CTD) signal motif, to the external environment
374 (27). The gene encoding the long fimbriae surface appendage, FimA, together with its accessory
375 proteins of the *fim* operon are under-expressed in excess hemin. The genes encoding regulatory
376 proteins (*e.g.* AraC, TetR (AcrR), and LuxR) follow a similar expression pattern. Many transposases
377 were also under-expressed in excess hemin, whereas no transposases were over-expressed in excess
378 hemin, suggesting that the expression of these mobile elements is a characteristic of a stress
379 environment where access to iron is limited.

380 We compared our results with two previous studies exploring expression (12) and proteomic (13)
381 differences in *P. gingivalis* according to hemin availability in the media. We observed that both
382 Anaya-Bergman *et al.* (2015) and Veith *et al.* (2018) previously reported changes in the expression of
383 the phosphomethylpyrimidine synthase ThiC, involved in thiamine biosynthesis, under excess hemin
384 conditions. Moreover, both studies also reported under-expressed levels of the genes coding
385 peroxiredoxin and a phosphotransferase. Separately, Anaya-Bergman *et al.* (2015) shared three
386 over-expressed genes with our study, *i.e.* the 2-iminoacetate synthase thiH, thiazole synthase thiG
387 and a thiamine phosphate synthase (W83: PG2109/HMPREF1322_RS02110), and Veith *et al.* (2018)
388 results matched three of the over-expressed genes identified by us, *i.e.* the rubrerythrin family
389 protein HMPREF1322_RS04040 (W83: PG0195) and two hypothetical proteins (W83:
390 PG0717/HMPREF1322_RS01045 and PG2105/HMPREF1322_RS02130). Veith *et. al* (2018) proteomic
391 results also identified proteins for 11 additional under-expressed genes found in our study. These
392 genes coded the cobaltochelatase subunit CobN (W83: PG1553/HMPREF1322_RS06780), the heme-
393 binding protein HmuY(W83: PG1551/HMPREF1322_RS06790), a histidinol phosphate phosphatase
394 (W83: PG0555/HMPREF1322_RS03860), a MMPL family transporter (W83:
395 PG1180/HMPREF1322_RS06005), a peroxiredoxin (W83: PG0618/HMPREF1322_RS06360), a
396 phosphoribosyltransferase (W83: PG1513/HMPREF1322_RS06960), a phosphotransferase (W83:
397 PG0456/HMPREF1322_RS00135), a T9SS type A sorting domain-containing protein (W83:
398 PG0495/HMPREF1322_RS03170), a TonB-dependent receptor (W83:
399 PG1552/HMPREF1322_RS06785), a transporter protein (W83: PG1626/HMPREF1322_RS06460) and
400 three hypothetical proteins (W83: PG0350/HMPREF1322_RS02675, W83:
401 PG0613/HMPREF1322_RS06380, W83: PG1555/HMPREF1322_RS06770). The
402 HMPREF1322_RS06770 hypothetical protein, the HMPREF1322_RS06360 peroxiredoxin and the
403 HMPREF1322_RS06460 transporter respectively matched the PG1555 MotA/TolQ/ExbB proton
404 channel family, PG0618 alkyl peroxide reductase AhpC and PG1626 FADL outer membrane receptor
405 protein annotated in *P. gingivalis* W83 strain genome.

406 Epigenetic mechanisms, including the methylation of specific DNA sequences by DNA
407 methyltransferases, allow unicellular organisms to respond rapidly to environmental stresses (28).
408 Here we showed that both adenines and cytosines can be differentially methylated in *P. gingivalis*
409 according to hemin availability in its microenvironment. Unlike in eukaryotes, in bacteria 5mC is not
410 the dominant DNA modification and instead exists alongside 4mC and 6mA, the latter being the
411 most prevalent modification in prokaryotes (29). Here we characterized both 6mA and 5mC and
412 verified higher levels of adenine methylation (mean = 23% and median = 13% for 6mA genome-wide)
413 in comparison to cytosine methylation (mean = 18% and median = 13% for 5mC genome-wide).
414 However, lack of previous DNA methylation studies in *P. gingivalis* and a general lack of knowledge
415 of the most common genetic motifs targeted by DNA methyltransferases (DNMTs) in this bacterium
416 limited the analyses that we could undertake, and may impact some of the interpretation of data.

417 We analysed DNA methylation changes in Dam/Dcm motifs (mean = 8% and median = 13% for Dam;
418 mean = 0.02% and median = 0% for Dcm genome-wide) to investigate possible Dam and Dcm-like
419 DNA methylation in *P. gingivalis*. However, we observed only limited evidence for Dam-like 'GATC'
420 methylation effects that overlapped differential gene expression. Alternatively, and because no
421 standard model for methylation calling in *P. gingivalis* exists, we used Nanopore reads and all-
422 context predictive models in Tombo to estimate the proportion of reads harbouring methylated
423 bases in our study. All-context models in turn introduced a higher degree of uncertainty in
424 methylation calling in our analysis. Additionally, we used proportion of methylated reads as an
425 estimate of methylation levels in each sample of bacterial cells. In our data most positions at which
426 DNA methylation was detected were not fully methylated or demethylated, pointing to presence of
427 heterogeneity in the level of DNA methylation across different bacterial cells from the same culture
428 sample (S8 and S9 Fig).

429 DNA methylation has historically been associated with bacterial DNA restriction-modification
430 systems, which protect bacterial cells from foreign DNAs (28). More recently DNA methylation has
431 also been shown to play important roles in other aspects of bacterial biology such as timing of DNA
432 replication, timing of transposition and conjugal transfer of plasmids, DNA repair and cell
433 partitioning, and regulation of gene expression (28). Less is known however about how widespread
434 the role of DNA methylation is in virulence and pathogenesis. Prior evidence suggests that the
435 activity of DNMTs such as Dam can for example affect virulence in a number of pathogens including
436 *Escherichia coli, Salmonella* spp., *Yersinia pseudotuberculosis* and *Vibrio cholerae* (30).

437 Here we showed that the availability of hemin – a critical micronutrient that modulates the
438 expression of virulence factors in *P. gingivalis* – is linked to changes in the DNA methylome of this
439 bacterium. We also showed that methylation changes were coordinated to alterations in the
440 expression of lactate utilization and ABC transporter genes, however their exact role in *P. gingivalis*
441 remains unknown. Previous research found that lactate utilization (in *Haemophilus influenzae and*
442 *Staphylococcus aureus*) and ABC transport of iron, manganese and/or zinc ions across the membrane
443 (*e.g.,* in *Yersinia pestis, Salmonella enterica* and *Streptococcus* spp.) is linked to increased virulence
444 (31-33). In our study, differential methylation in lactate utilization and ABC transporter genes co-
445 occurred with their decreased expression in excess hemin conditions. We hypothesize that the
446 decreased expression of these genes in excess hemin, and conversely their relatively increased
447 expression in limited hemin, could be related to *P. gingivalis* scavenging of nutrients according to
448 their availability in the growth environment.

449 In conclusion, using Nanopore sequencing we were able to characterise for the first time the
450 epigenetic landscape of *P. gingivalis* W50, and to compare epigenetic variation to changes in gene
451 expression. We showed that iron availability in the bacterium's microenvironment can lead to
452 discrete DNA methylation changes potentially impacting the expression of genes related to growth
453 and virulence in humans. There is, however, a need to better characterise the diversity of motifs
454 targeted by different DNMTs, including from *P. gingivalis.* A more comprehensive characterisation of
455 DNMTs and their targeted motifs in the bacterial world will allow better future exploring of DNA
456 methylation in *P. gingivalis* with Oxford Nanopore.

457

Materials and methods

Continuous culturing conditions

Strain Culture

P. gingivalis W50 was cultured on Columbia blood agar (CBA; Oxoid) supplemented with 5% oxalated horse blood (Oxoid) incubated anaerobically (5% CO_2/5% H_2/90% N_2) at 37°C for 72 hours. A single colony was inoculated into 100 mL of pre-reduced Brain Heart Infusion (BHI; Oxoid) broth supplemented with 5 mg L^{-1} filter sterilised (0.22 µM) hemin and incubated until late log phase (48-72 hours).

Continuous Culture Chemostat Configuration

A one litre, sealed glass chemostat was autoclave sterilised with 300 mL BHI *in situ*. 100 mL of *P. gingivalis* culture was inoculated into the chemostat through a designated inoculation tube, using a peristaltic pump (Watson Marlow 101U). Sterile BHI (supplemented with either 0.2 or 5 mg L^{-1} hemin for limited and excess conditions, respectively) was continuously fed at a flow rate of 20 mL h^{-1} to achieve the working volume of 700 mL, before being increased to 70 mL h^{-1}, in conjunction with harvest/waste pump activation at the equivalent rate. These conditions set a fixed dilution rate of 0.1 h^{-1} which corresponds to constant mean generation time of 6.9 h. Steady state conditions were achieved after approximately 10 mean generations. Environmental conditions were controlled/monitored using an Applikon ADI 1030 Bio-controller and BioXpert V2 software (Applikon Biotechnology, The Netherlands). The pH of the culture was maintained automatically at pH7±0.1 using 1 M NaOH and 0.5 M HCl fed through a peristaltic pump. Temperature was preserved at 37 ± 0.3°C with a silicon heat jacket. The chemostat was continuously sparged with filter-sterilised 5% CO_2/95% N_2 to maintain anaerobic conditions and stirred at 40 rpm (Motor Controller ADI 1012, Applikon Biotechnology) (S10 Fig).

Experimental Design

Two independent chemostat experiments were performed, one fed with 5 mg L^{-1} hemin (excess) and one fed with 0.2 mg L^{-1} hemin (limitation). Post-inoculation, the optical density (OD_{600}) of the culture was monitored every 12 hours using a benchtop spectrophotometer (Jenway 6305). Steady state was defined as three consecutive OD_{600} readings within 10% of each other. Total viable counts and culture purity were determined daily, following serial dilutions in phosphate buffered saline, inoculation of CBA plates in triplicates and growth in a Whitley A45 anaerobic Workstation (Don Whitley Scientific, UK). Sampling for DNA and RNA analysis was performed every 48 hours during steady state (**Error! Reference source not found.**1). This represented biological replicates separated by five full volume replenishments of the chemostat vessel.

Nucleic Acid Sampling

During nucleic acid sampling periods the harvest bottle was replaced with a sterile collection bottle (on ice) and approximately 20 mL was collected. For DNA sampling, 1 mL aliquots were centrifuged at 13,000 rpm for 10 minutes (4°C), prior to supernatant removal and storage at −80°C. For RNA samples, ten 1 mL samples were similarly centrifuged, the supernatant decanted, and the pellet reconstituted in 1mL of DNA/RNA Shield (Zymo Research, USA), prior to storage at −80°C.

DNA extraction

One mL cultures were centrifuged at 17,000×g, at 4°C for 10 minutes. The pellets were used to extract high molecular weight DNA using Gentra Puregene yeast/bacteria DNA isolation kit (Qiagen),

500 following the manufacturer's protocol. DNA was finally resuspended in 200 µl EB buffer (Qiagen) and
501 stored at 4°C before use.

502 RNA extraction

503 Cells were pelleted as above and resuspended/lysed in 350 µl of DNA/RNA Shield (Cambridge
504 Biosciences) at room temperature. The solutions were used directly in RNA isolation with Zymo
505 Quick-RNA™ miniprep kit (Cambridge Biosciences) in accordance with the manufacture's protocol.
506 This incorporated the initial chromosomal DNA removal, and on-column DNAase I digestion before
507 the final wash and elution into 50 µl nuclease-free water. RNA was stored at −70°C.

508 Illumina RNA sequencing

509 RNA samples were first subjected to rRNA depletion using the NEBNext® rRNA Depletion Kit
510 (Bacteria). The samples were then used for RNA-seq library preparation using the NEBNext Ultra II
511 Directional RNA Library Prep Kit for Illumina. Both kits were used according to the manufacturer's
512 instructions. Sequencing was performed by Novagene, UK on an Illumina Novaseq6000 instrument.

513 Oxford Nanopore DNA sequencing

514 MinIon library preparation and DNA sequencing was performed at the University of Nottingham on
515 MinIon flow cell (Oxford Nanopore). Whole-genome sequencing libraries were prepared from six
516 bacterial genomic DNA samples. DNA samples were quantified using the Qubit 4 Fluorometer
517 (Thermo Fisher Scientific) and the Qubit dsDNA BR Assay Kit (Thermo Fisher Scientific; Q32853) and
518 the Agilent 4200 TapeStation and the Agilent Genomic DNA ScreenTape Assay (Agilent; 5067-5365
519 and 5067-5366) were used to assess the molecular weight of the DNA. Sequencing libraries were
520 prepared using the Native barcoding genomic DNA protocol (Oxford Nanopore Technologies;
521 Version: NBE_9065_v109_revS_14Aug2019). This protocol uses the Ligation Sequencing Kit (Oxford
522 Nanopore Technologies; SQK-LSK109) and the Native Barcoding Expansion 1-12 kit (Oxford
523 Nanopore Technologies; EXP-NBD104) to barcode the unsheared DNA fragments within each
524 sample. Barcoded samples were then pooled in equimolar amounts for the final sequencing adapter
525 ligation. All purification steps were performed using AMPure XP beads (Beckman Coulter; A63882).
526 The final barcoded library pool was loaded onto a MinION flow cell (Oxford Nanopore Technologies;
527 FLO-MIN106 R9.4.1) and run on the GridION X5 Mk1.

528 Bioinformatic analyses

529 RNA sequencing data processing

530 Sequencing data was processed using the ProkSeq pipeline v2.8 (22) Briefly, FastQC (34)and AfterQC
531 (35, 36) were implemented to check the quality of data, trim adaptor sequences and filter out low
532 quality reads using standard parameters. This resulted in a total of ≈25.3–36.0 M PE reads (2 × 76
533 bp) being kept for downstream processing. Subsequently, bowtie2 (35) was used to align reads
534 against the 104 contigs of the *P. gingivalis* W50 genome assembly deposited in the NCBI RefSeq
535 (accession no. GCF_000271945.1). RefSeq gene annotations were extracted from *P. gingivalis*' GTF
536 file and the number of total reads per gene were calculated using featureCounts (37). Counts per
537 gene were estimated for 1992 genes. RSeQC (38) was used to study sample coverage uniformity
538 along the body of genes.

539 DNA methylation calling

540 *Motif-dependent DNA methylation calling*

541 Modified basecalling was first performed with Guppy v3.2.10+aabd4ec (Oxford Nanopore) using the
542 high accuracy methylation aware configuration available for Dam and Dcm motifs from *Escherichia*

543 *coli* ('dna_r9.4.1_450bps_modbases_dam-dcm-cpg_hac.cfg'). Total Nanopore read data included
544 ≈240–380 K reads (88 bp – 143 kb, N50 = 27 kb) per sample. Methylated and canon bases were then
545 aggregated against the *P. gingivalis* W50 reference genome using Medaka v0.11.5
546 (*https://github.com/nanoporetech/medaka*). Base counts were normalized for the total number of
547 reads in each sample × 10,000 reads in similar fashion to the RPG10K method (39, 40). The
548 proportion of methylated bases to the total number of bases (methylated + canon bases) was
549 estimated at each genomic motif and motifs were filtered for minimum 10× coverage across
550 samples. A total of 12,066 'GATC' (Dam), 419 'CCAGG' (Dcm) and 400 'CCTGG' (Dcm) motifs were
551 kept for downstream analyses.

552 ### *Motif-independent DNA methylation calling*

553 Nanopore signals were originally stored in multi-read fast5 files and the *ont_fast5_api*
554 'multi_to_single_fast5' (*https://github.com/nanoporetech/ont_fast5_api*) was used to generate
555 single fast5 files before detection of non-standard nucleotides with Tombo v1.5.1 (41). First, electric
556 current signal level data was re-squiggled using the same *P. gingivalis* W50 reference genome used
557 to pre-process the RNA-Seq and methylated motif data. Secondly, all-context motif-independent
558 models were used in Tombo to detect the alternative bases 6mA and 5mC from the signal data.
559 Alternative base calling in each sample was summarized per genomic position with coverage and
560 dampened fractions estimated at each adenine and cytosine site of both positive and negative DNA
561 strands. Coverage was stored in the bedGraph format and proportion of methylation in the WIG
562 format. Data files were imported into R using the package *rtracklayer* (42) and combined into a
563 single data frame using GRanges, IRanges and *findOverlaps* from the IRanges package (43).

564 The proportion of methylation – dampened fraction – was estimated by adjusting the proportion of
565 methylated reads according to coverage at low coverage sites in order to include them in
566 downstream analyses (41). Despite this, only adenines and cytosines with at least 10× coverage
567 across samples were included in our analysis here as well. Overall, 1,150,659 adenines and 1,079,809
568 cytosines were kept for downstream analyses, with 350–525× mean base coverage per sample.

569 ## Statistical analyses

570 ### Differential gene expression analysis

571 DESeq2 (23) was used to normalize the read count data and perform differential gene expression
572 analysis. Growth in limited hemin was the 'control' and growth in excess hemin was the 'treatment'.
573 All three samples from each condition were used and global sample differences were observed using
574 the principal component analysis method. Both DESeq2 and edgeR (44) were implemented from
575 ProkSeq's downstream analysis. Both methods allow for inter-sample comparison in differential
576 gene expression analysis. Here we used edgeR results as sensitivity for DESeq2 results since edgeR
577 normalizes expression data differently to DESeq2 (DESeq2 uses the median of ratios method and
578 edgeR uses the trimmed mean of M values to normalize read count data). The false discovery rate
579 method (FDR) was used to identify differentially expressed genes and genes with FDR < 5% and a
580 $\log_2$ fold change (LFC) > 1.5 or < −1.5 were respectively considered over and under-expressed in
581 excess hemin. Differentially expressed genes were subsequently manually annotated to the *P.*
582 *gingivalis* W83 genome (GenBank accession no. AE015924) (25) in order to compare results with
583 previous research. Synteny analysis at specific loci was performed using MAUVE (45).

584 ### Gene ontology enrichment analysis

585 Gene ontology (GO) enrichment analysis in over and under-expressed gene sets was performed
586 using ShinyGO (46). Because the genome of *P. gingivalis* W50 was not available from ShinyGO's

587 species database, only well-characterized genes that matched gene symbols in *P. gingivalis* W83
588 reference strain genome were used in this analysis. A more relaxed FDR threshold of 10% was
589 applied to assess enrichment in this case and GO molecular functions were reported.

590 Differential DNA methylation analysis

591 Mean and median DNA methylation across samples were calculated using all motifs, adenines and
592 cytosines kept for downstream analysis. Global DNA methylation differences between the samples
593 were observed using principal component analysis for Dam/Dcm and all-context 6mA and 5mC
594 modifications, selecting for minimum 10× and 100× coverage per position.

595 Two-sided Student's t-tests were applied at each motif, adenine and cytosine site after filtering for
596 positions where at least a 5% mean methylation difference was observed between the experimental
597 conditions (79 'GATC' motifs (Dam), 139,794 all-context adenines and 87,398 all-context cytosines).
598 A sensitivity analysis was performed for minimum 100× coverage (66 'GATC' motifs (Dam), 85,090
599 all-context adenines and 46,930 all-context cytosines) to ascertain whether the significance of
600 results was impacted by depth of sequencing. Results were considered statistically significant at an
601 FDR threshold of 5% to match gene expression analysis.

602 The differentially methylated motifs and all-context positions identified were annotated to nearby
603 genes considering the location and gene strand. First, 'GATC'-DMMs, DMAs and DMCs were
604 annotated to the gene they were located if present in the gene body, and secondly, they were
605 annotated to genes found in the same contig and within ±1kb of their location. Genes located in the
606 opposite strand of the methylation signal were considered in both cases.

607 In comparing the overlap between DEGs, DMA, DMCs and 'GATC'-DMMs we considered all DMAs,
608 DMCs and 'GATC'-DMMs that were in or near the gene (±1 kb away, both strands). DMA and DMC
609 data were further used to test the wider DNA methylation effects on the expression of nearby genes.
610 A contingency table containing all 1192 genes was constructed and Fischer's exact tests were
611 employed to test for the enrichment of genes with concurrent gene expression and all-context DNA
612 methylation changes. The enrichment of differential DNA methylation directly upstream,
613 downstream and in the body of genes was also tested. Here, Wilcoxon signed-rank tests were used
614 to test for generalized shifts in DNA methylation signals between the experimental conditions 100
615 bp upstream, 100 bp downstream and within the body of genes previously annotated to DMAs
616 and/or DMCs.

617 Motif enrichment analysis

618 The MEME (Multiple EM for Motif Elicitation) online tool (47) was used to detect enriched motifs
619 containing the DMAs and DMCs identified with concurrent gene expression changes. For this, 15
620 base pair long DNA sequences surrounding the DMAs and DMCs identified were extracted.
621 Subsequently, motifs with minimum 4 bp and maximum 15 bp were searched using MEME's Classic
622 objective function and the ZOOPS distribution model. Both the given strand and the reverse
623 complement strand were considered, and the top 10 motifs found were reported. Motifs were
624 considered significant if their reported E-value threshold was ≤ 0.05.

625

626 Acknowledgments

627 We are grateful to the Medical Research Council of United Kingdom for the grant: MR/P012175/2.
628 We thank the teams at the genome sequencing centres for assistance, and Mr Darioush Yarand and

the Rosalind KCL high performance Linux cluster system administration team for help resolving file space and software installation queries.

Author contributions

MAC and VR conceptualized the study. MAC, VR, DAD and JTB provided resources. MAC, VR, and JTB supervised the study. RC and JA-O implemented the methodology, JA-O performed experiments, and RC carried out formal analysis and software implementation. JJV, FR-A, SJ, DAD, PDM, and VR contributed to methodology, experiments, analysis, and results interpretation. RC, JA-O, MAC, and JTB drafted the manuscript, and all authors reviewed and edited the manuscript.

References

1. Curtis MA, Zenobia C, Darveau RP. The relationship of the oral microbiotia to periodontal health and disease. Cell Host Microbe. 2011;10(4):302-6.
2. Curtis MA, Diaz PI, Van Dyke TE. The role of the microbiota in periodontal disease. Periodontol 2000. 2020;83(1):14-25.
3. Dominy SS, Lynch C, Ermini F, Benedyk M, Marczyk A, Konradi A, et al. in Alzheimer's disease brains: Evidence for disease causation and treatment with small-molecule inhibitors. Sci Adv. 2019;5(1):eaau3333.
4. Sedghi LM, Bacino M, Kapila YL. Periodontal Disease: The Good, The Bad, and The Unknown. Front Cell Infect Microbiol. 2021;11:766944.
5. Hajishengallis G. Interconnection of periodontal disease and comorbidities: Evidence, mechanisms, and implications. Periodontol 2000. 2022.
6. Hajishengallis G, Liang S, Payne MA, Hashim A, Jotwani R, Eskan MA, et al. Low-abundance biofilm species orchestrates inflammatory periodontal disease through the commensal microbiota and complement. Cell Host Microbe. 2011;10(5):497-506.
7. Payne MA, Hashim A, Alsam A, Joseph S, Aduse-Opoku J, Wade WG, et al. Horizontal and Vertical Transfer of Oral Microbial Dysbiosis and Periodontal Disease. J Dent Res. 2019;98(13):1503-10.
8. Lunar Silva I, Cascales E. Molecular Strategies Underlying *Porphyromonas gingivalis* Virulence. J Mol Biol. 2021;433(7):166836.
9. Haurat MF, Aduse-Opoku J, Rangarajan M, Dorobantu L, Gray MR, Curtis MA, et al. Selective sorting of cargo proteins into bacterial membrane vesicles. J Biol Chem. 2011;286(2):1269-76.
10. Smalley JW, Thomas MF, Birss AJ, Withnall R, Silver J. A combination of both arginine- and lysine-specific gingipain activity of *Porphyromonas gingivalis* is necessary for the generation of the micro-oxo bishaem-containing pigment from haemoglobin. Biochem J. 2004;379(Pt 3):833-40.
11. Smalley JW, Olczak T. Heme acquisition mechanisms of *Porphyromonas gingivalis* - strategies used in a polymicrobial community in a heme-limited host environment. Mol Oral Microbiol. 2017;32(1):1-23.
12. Anaya-Bergman C, Rosato A, Lewis JP. Iron- and hemin-dependent gene expression of *Porphyromonas gingivalis*. Mol Oral Microbiol. 2015;30(1):39-61.
13. Veith PD, Luong C, Tan KH, Dashper SG, Reynolds EC. Outer Membrane Vesicle Proteome of *Porphyromonas gingivalis* Is Differentially Modulated Relative to the Outer Membrane in Response to Heme Availability. J Proteome Res. 2018;17(7):2377-89.
14. Lamont RJ, Jenkinson HF. Life below the gum line: pathogenic mechanisms of *Porphyromonas gingivalis*. Microbiol Mol Biol Rev. 1998;62(4):1244-63.

674 15. Curtis MA, Aduse Opoku J, Rangarajan M, Gallagher A, Sterne JA, Reid CR, et al. Attenuation
675 of the virulence of *Porphyromonas gingivalis* by using a specific synthetic Kgp protease inhibitor.
676 Infect Immun. 2002;70(12):6968-75.
677 16. McKee AS, McDermid AS, Baskerville A, Dowsett AB, Ellwood DC, Marsh PD. Effect of hemin
678 on the physiology and virulence of *Bacteroides gingivalis* W50. Infect Immun. 1986;52(2):349-55.
679 17. Mattos-Graner RO, Duncan MJ. Two-component signal transduction systems in oral bacteria.
680 J Oral Microbiol. 2017;9(1):1400858.
681 18. Jiang C, Yang D, Hua T, Hua Z, Kong W, Shi Y. A PorX/PorY and σ^P Feedforward
682 RegulatoryLoop Controls Gene Expression Essential for *Porphyromonas gingivalis* Virulence.
683 mSphere. 2021;6(3):e0042821.
684 19. Yang D, Jiang C, Ning B, Kong W, Shi Y. The PorX/PorY system is a virulence factor of
685 *Porphyromonas gingivalis* and mediates the activation of the type IX secretion system. J Biol Chem.
686 2021;296:100574.
687 20. Murphy TR, Xiao R, Hamilton-Brehm SD. Hybrid genome de novo assembly with methylome
688 analysis of the anaerobic thermophilic subsurface bacterium *Thermanaerosceptrum fracticalcis*
689 strain DRI-13T. BMC Genomics. 2021;22(1):209.
690 21. Tourancheau A, Mead EA, Zhang XS, Fang G. Discovering multiple types of DNA methylation
691 from bacteria and microbiome using nanopore sequencing. Nat Methods. 2021;18(5):491-8.
692 22. Firoj Mahmud AKM, Delhomme N, Nandi S, Fällman M. ProkSeq for complete analysis of
693 RNA-Seq data from prokaryotes. Bioinformatics. 2020.
694 23. Love MI, Huber W, Anders S. Moderated estimation of fold change and dispersion for RNA-
695 seq data with DESeq2. Genome Biol. 2014;15(12):550.
696 24. Kondo Y, Ohara N, Sato K, Yoshimura M, Yukitake H, Naito M, et al. Tetratricopeptide repeat
697 protein-associated proteins contribute to the virulence of *Porphyromonas gingivalis*. Infect Immun.
698 2010;78(6):2846-56.
699 25. Nelson KE, Fleischmann RD, DeBoy RT, Paulsen IT, Fouts DE, Eisen JA, et al. Complete
700 genome sequence of the oral pathogenic Bacterium *Porphyromonas gingivalis* strain W83. J
701 Bacteriol. 2003;185(18):5591-601.
702 26. Sztukowska M, Bugno M, Potempa J, Travis J, Kurtz DM. Role of rubrerythrin in the oxidative
703 stress response of *Porphyromonas gingivalis*. Mol Microbiol. 2002;44(2):479-88.
704 27. Veith PD, Glew MD, Gorasia DG, Reynolds EC. Type IX secretion: the generation of bacterial
705 cell surface coatings involved in virulence, gliding motility and the degradation of complex
706 biopolymers. Mol Microbiol. 2017;106(1):35-53.
707 28. Casadesús J, Low D. Epigenetic gene regulation in the bacterial world. Microbiol Mol Biol
708 Rev. 2006;70(3):830-56.
709 29. Beaulaurier J, Schadt EE, Fang G. Deciphering bacterial epigenomes using modern
710 sequencing technologies. Nat Rev Genet. 2019;20(3):157-72.
711 30. Low DA, Weyand NJ, Mahan MJ. Roles of DNA adenine methylation in regulating bacterial
712 gene expression and virulence. Infect Immun. 2001;69(12):7197-204.
713 31. Garmory HS, Titball RW. ATP-binding cassette transporters are targets for the development
714 of antibacterial vaccines and therapies. Infect Immun. 2004;72(12):6757-63.
715 32. Fuller JR, Vitko NP, Perkowski EF, Scott E, Khatri D, Spontak JS, et al. Identification of a
716 lactate-quinone oxidoreductase in *Staphylococcus aureus* that is essential for virulence. Front Cell
717 Infect Microbiol. 2011;1:19.
718 33. Lichtenegger S, Bina I, Roier S, Bauernfeind S, Keidel K, Schild S, et al. Characterization of
719 lactate utilization and its implication on the physiology of *Haemophilus influenzae*. Int J Med
720 Microbiol. 2014;304(3-4):490-8.
721 34. Wingett SW, Andrews S. FastQ Screen: A tool for multi-genome mapping and quality control.
722 F1000Res. 2018;7:1338.
723 35. Langmead B, Salzberg SL. Fast gapped-read alignment with Bowtie 2. Nat Methods.
724 2012;9(4):357-9.

725 36. Chen S, Huang T, Zhou Y, Han Y, Xu M, Gu J. AfterQC: automatic filtering, trimming, error
726 removing and quality control for fastq data. BMC Bioinformatics. 2017;18(Suppl 3):80.
727 37. Liao Y, Smyth GK, Shi W. featureCounts: an efficient general purpose program for assigning
728 sequence reads to genomic features. Bioinformatics. 2014;30(7):923-30.
729 38. Wang L, Wang S, Li W. RSeQC: quality control of RNA-seq experiments. Bioinformatics.
730 2012;28(16):2184-5.
731 39. Byrne A, Beaudin AE, Olsen HE, Jain M, Cole C, Palmer T, et al. Nanopore long-read RNAseq
732 reveals widespread transcriptional variation among the surface receptors of individual B cells. Nat
733 Commun. 2017;8:16027.
734 40. Bayega A, Oikonomopoulos S, Gregoriou ME, Tsoumani KT, Giakountis A, Wang YC, et al.
735 Nanopore long-read RNA-seq and absolute quantification delineate transcription dynamics in early
736 embryo development of an insect pest. Sci Rep. 2021;11(1):7878.
737 41. Stoiber M, Quick J, Egan R, Eun Lee J, Celniker S, Neely RK, et al. *De novo* Identification of
738 DNA Modifications Enabled by Genome-Guided Nanopore Signal Processing. bioRxiv. 2022:094672.
739 42. Lawrence M, Gentleman R, Carey V. rtracklayer: an R package for interfacing with genome
740 browsers. Bioinformatics. 2009;25(14):1841-2.
741 43. Lawrence M, Huber W, Pagès H, Aboyoun P, Carlson M, Gentleman R, et al. Software for
742 computing and annotating genomic ranges. PLoS Comput Biol. 2013;9(8):e1003118.
743 44. Robinson MD, McCarthy DJ, Smyth GK. edgeR: a Bioconductor package for differential
744 expression analysis of digital gene expression data. Bioinformatics. 2010;26(1):139-40.
745 45. Darling AE, Mau B, Perna NT. progressiveMauve: multiple genome alignment with gene gain,
746 loss and rearrangement. PLoS One. 2010;5(6):e11147.
747 46. Ge SX, Jung D, Yao R. ShinyGO: a graphical gene-set enrichment tool for animals and plants.
748 Bioinformatics. 2020;36(8):2628-9.
749 47. Bailey TL, Williams N, Misleh C, Li WW. MEME: discovering and analyzing DNA and protein
750 sequence motifs. Nucleic Acids Res. 2006;34(Web Server issue):W369-73.

751

752 Supporting information

753 **S1 Fig.** Overlap between DeSeq2 and edgeR results for differentially expressed *P. gingivalis* genes
754 cultured in excess hemin conditions.

755 **S2 Fig.** DESeq2-normalized counts PCA for *P. gingivalis* growth in limited (red) and excess (blue)
756 hemin conditions.

757 **S3 Fig.** All-context DNA methylation PCA for *P. gingivalis* growth in limited (LiH) and excess (ExH)
758 hemin conditions, selecting for minimum 10× (A) and 100× (B) coverage.

759 **S4 Fig.** Dam/Dcm DNA methylation PCA for *P. gingivalis* growth in limited (LiH) and excess (ExH)
760 hemin conditions, selecting for minimum 10× (A) and 100× (B) coverage.

761 **S5 Fig.** MEME motif analysis results for the 49 and 47 DMAs and DMCs identified in the main
762 analysis.15-nucleotide long sequences surrounding DMAs and DMCs were extracted, and motifs
763 were analysed considering minimum and maximum motif widths of 4 and 15 nucleotides,
764 respectively. A maximum number of 10 motifs were searched. No motifs reached significance (E-
765 value < 0.05).

766 **S6 Fig.** Adenine methylation patterns upstream (−100 bp), downstream (+100 bp) and in the gene
767 body of differentially expressed genes annotated to DMAs. Differential methylation significance was
768 tested using Wilcoxon signed-rank tests between limited (red) and excess (blue) hemin conditions.

769 **S7 Fig.** Cytosine methylation patterns upstream (−100 bp), downstream (+100 bp) and in the gene
770 body of differentially expressed genes annotated to DMAs. Differential methylation significance was
771 tested using Wilcoxon signed-rank tests between limited (red) and excess (blue) hemin conditions.

772 **S8 Fig.** Distribution of all-context DNA methylation for *P. gingivalis* growth in limited (LiH) and excess
773 (ExH) hemin conditions, selecting for 10× (A) and 100× (B) coverage.

774 **S9 Fig.** Distribution of Dam/Dcm DNA methylation for *P. gingivalis* growth in limited (LiH) and excess
775 (ExH) hemin conditions, selecting for 10× (A) and 100× (B) coverage.

776 **S10 Fig.** Schematic representation of chemostat set up in class II fume cabinet.

777 **S1 Table.** Genes over-expressed in excess hemin conditions (>1.5 LFC, FDR = 5%).

778 **S2 Table.** Genes under-expressed in excess hemin conditions (<−1.5 LFC, FDR = 5%).

779 **S3 Table.** GO molecular functions over-expressed in excess hemin conditions (based on 40 genes,
780 FDR = 10%).

781 **S4 Table.** GO molecular functions under-expressed in excess hemin conditions (based on 8 genes,
782 FDR = 10%).

783 **S5 Table.** 'GATC'-DMMs identified in *P. gingivalis* W50, selecting for minimum 10× coverage and
784 mean 5% methylation difference between experimental conditions (FDR = 5%).

785 **S6 Table.** 'GATC'-DMMs identified in *P. gingivalis* W50, selecting for minimum 100× coverage and
786 mean 5% methylation difference between experimental conditions (FDR = 5%).

787 **S7 Table.** DMAs (6mA) identified in *P. gingivalis* W50, selecting for minimum 100× coverage and
788 mean 5% methylation difference between experimental conditions (FDR = 5%).

789 **S8 Table.** DMCs (5mC) identified in *P. gingivalis* W50, selecting for minimum 100× coverage and
790 mean 5% methylation difference between experimental conditions (FDR = 5%).

791 **S9 Table.** Genes over-expressed in excess hemin conditions with 'GATC'-DMMs (> 1.5 LFC, > 5%
792 methylation difference, FDR = 5%).

793 **S10 Table.** Genes under-expressed in excess hemin conditions with 'GATC'-DMMs (> 1.5 LFC, > 5%
794 methylation difference, FDR = 5%).

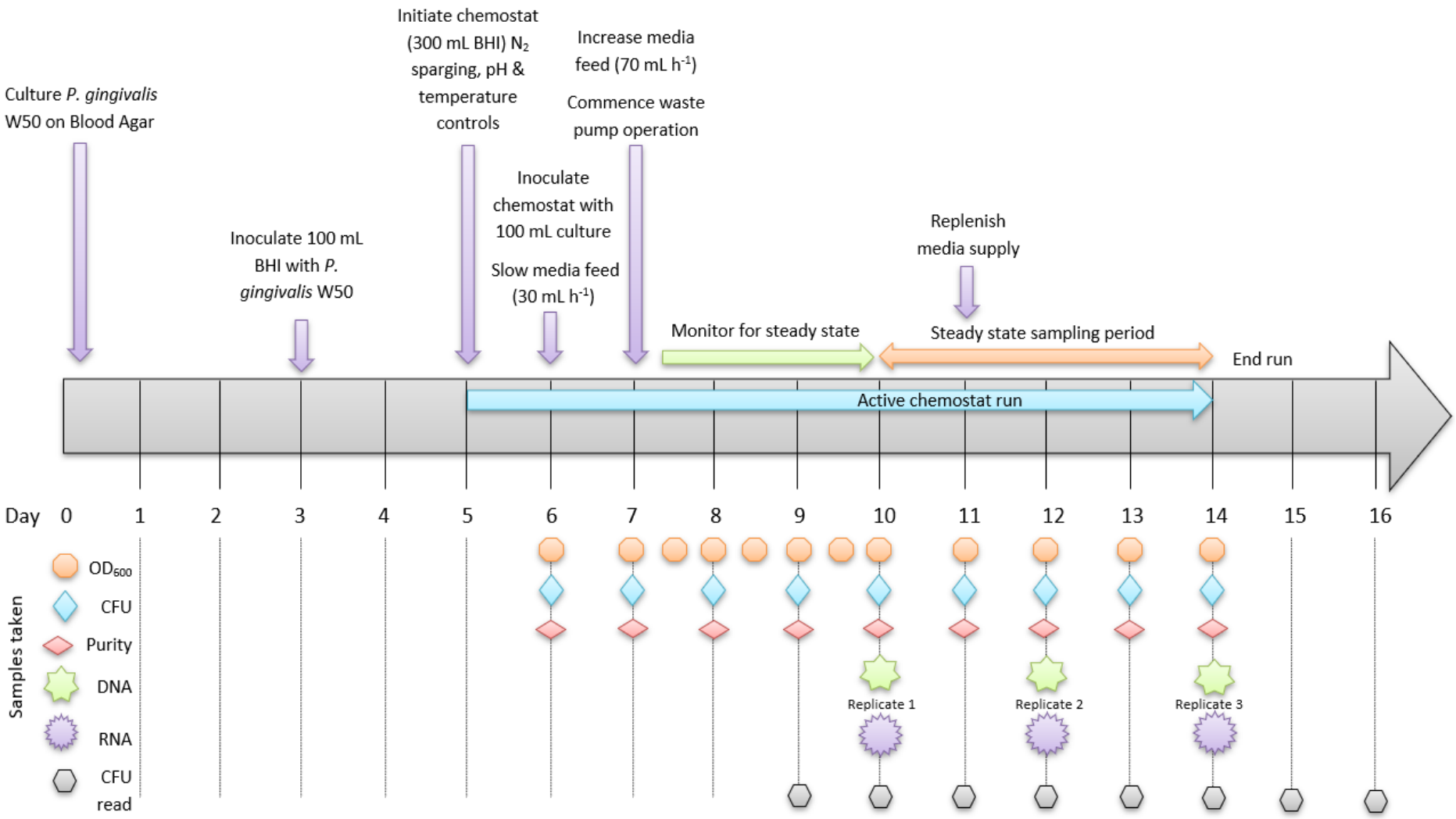

Fig 1. Timeline of *P. gingivalis* W50 chemostat operation and experimental design. CFU – colony forming unit, BHI – Brain Heart Infusion.

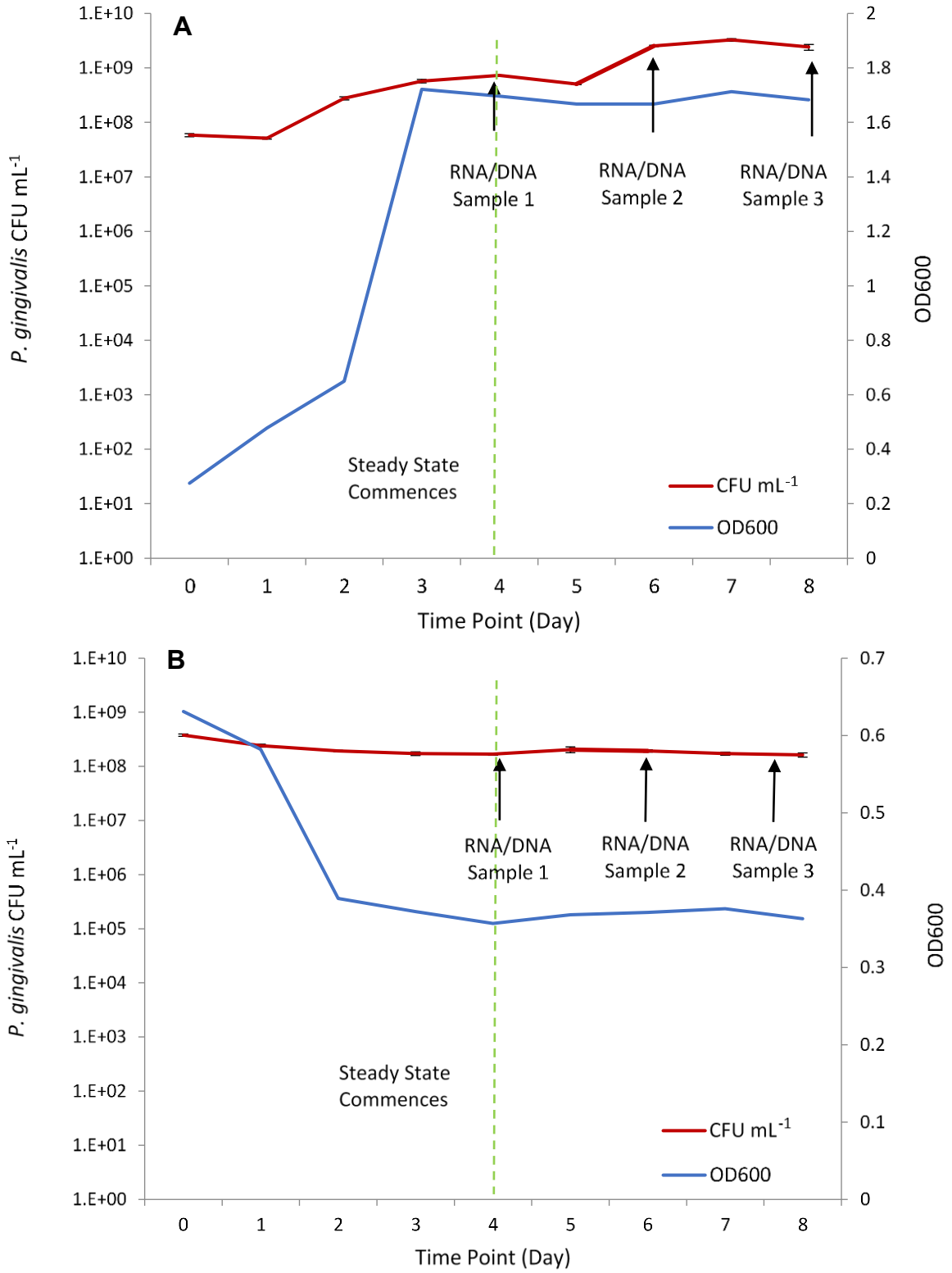

Fig 2. Enumeration of *P. gingivalis* populations throughout the continuous culture chemostat experimental duration by colony count and optical density (OD). A – *P. gingivalis* W50 cultured with excess hemin (5 mg L-1). B – *P. gingivalis* W50 cultured with limited hemin (0.2 mg L-1). CFU – colony forming units. Error bars represent standard error of the mean.

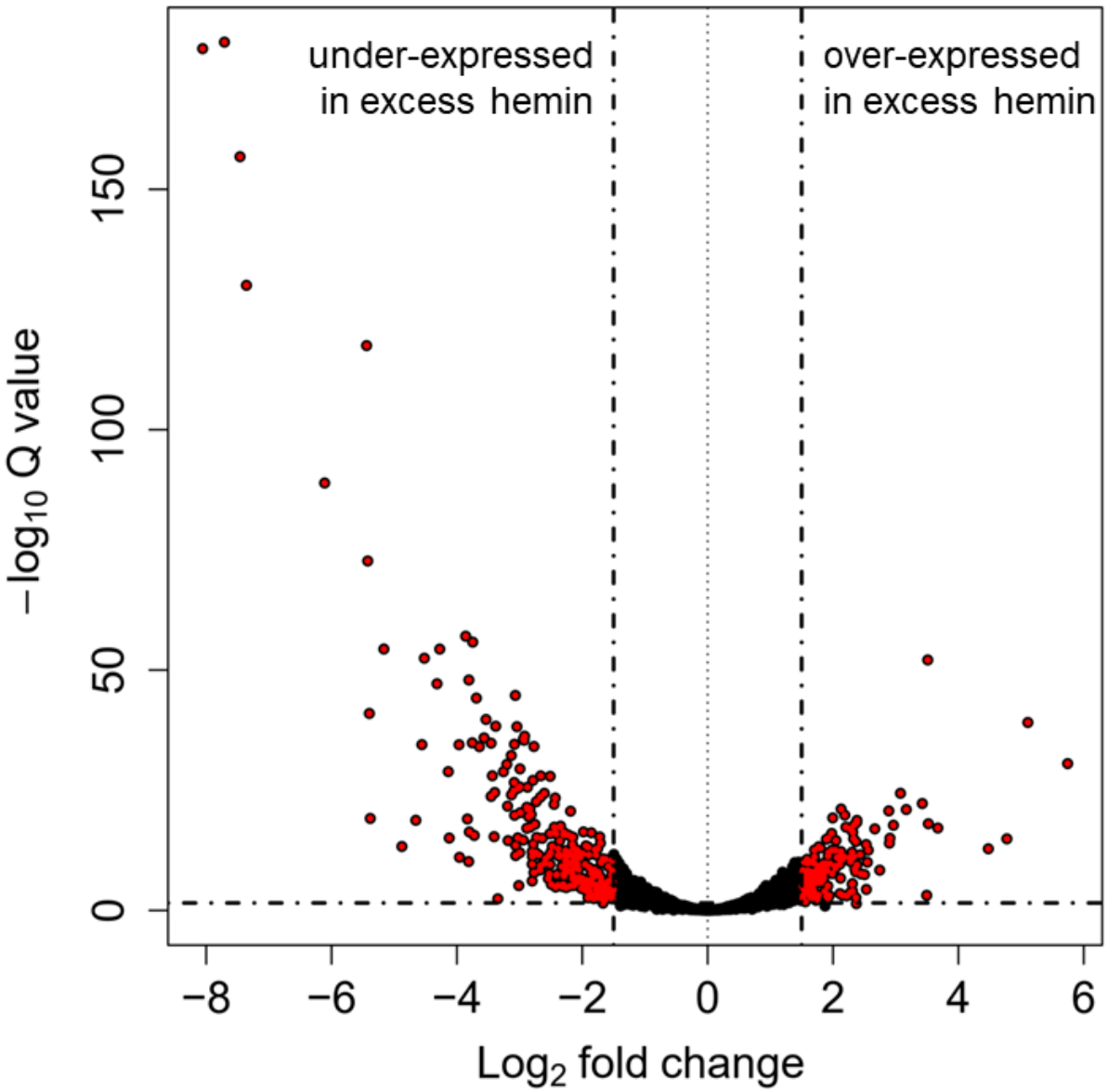

Fig 3. Differentially expressed genes in excess hemin conditions. *P. gingivalis* genes were considered differentially expressed if transcript abundance surpassed 1.5 LFC between culturing conditions (FDR = 5%).

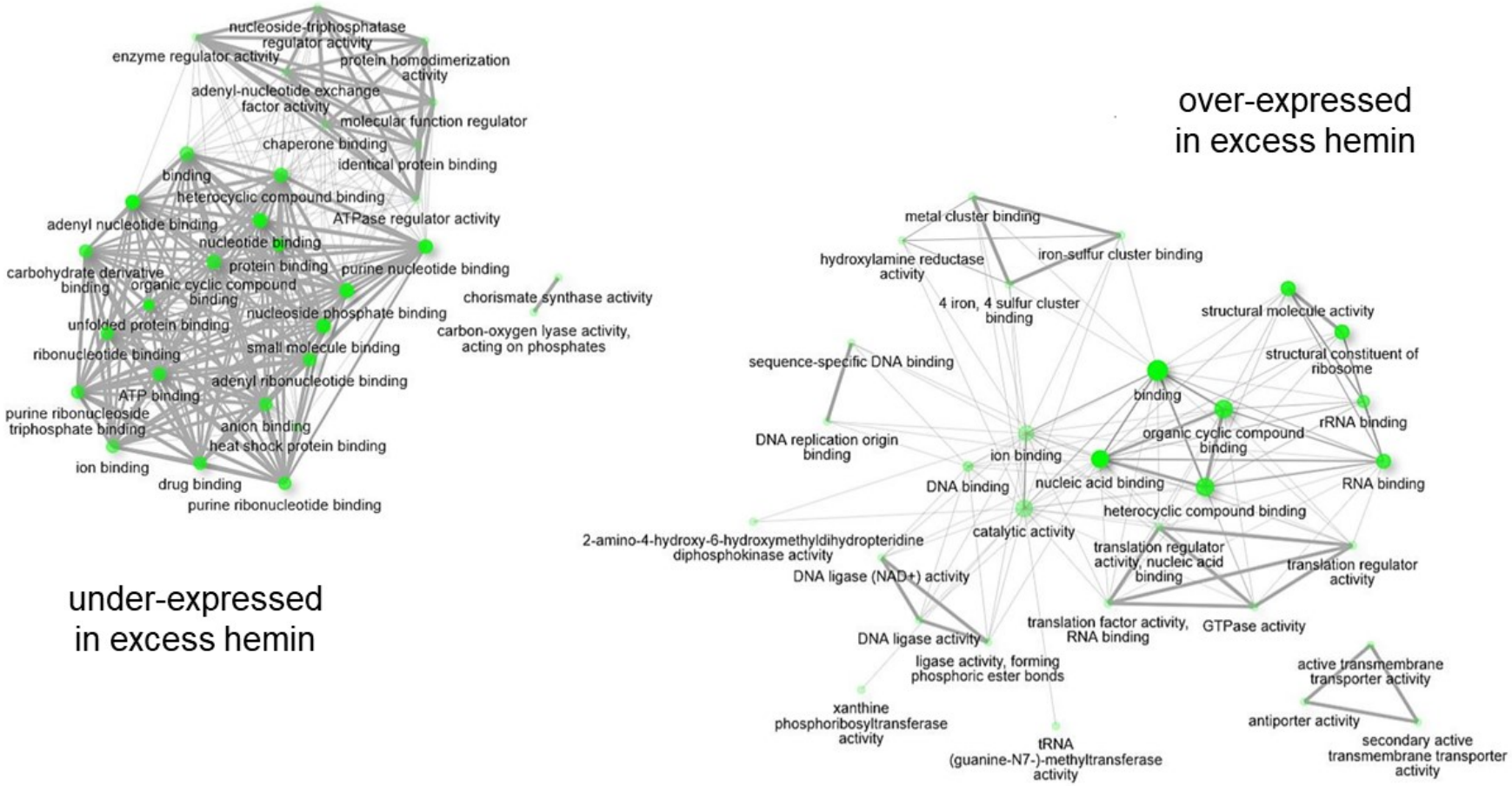

Fig 4. GO molecular function enrichment of genes under and over-expressed in excess hemin conditions (1.5 LFC, FDR = 10%). The top 30 GO molecular functions were selected to create the networks and edges represent pathways with > 10% shared genes. Darker nodes are more significantly enriched, bigger nodes represent larger gene sets and thicker edges correspond to more overlaps between gene sets. Pathways were created based on gene matches to *P. gingivalis* W83 reference genome.

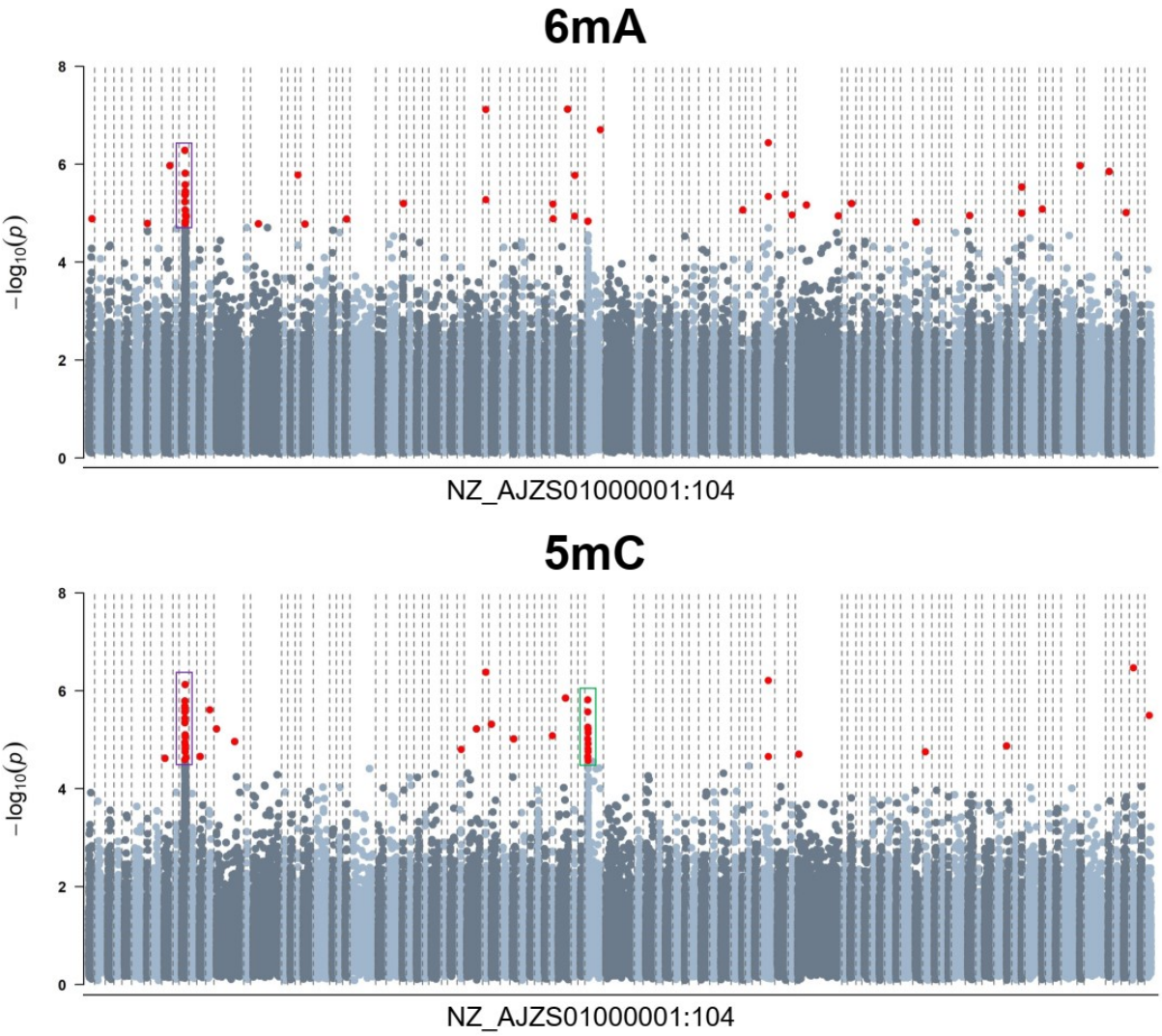

Fig 5. Differential methylation analysis results for excess hemin. Results are presented for 139,794 adenines (6mA) and 87,398 cytosines (5mC) showing a minimum 5% mean methylation difference between experimental conditions. Contigs were plotted in ascending order (NZ_AJZS01000001:104) and are delimited by the dashed lines in the graph. Genomic positions surpassing the FDR = 5% significance threshold are depicted in red. Clusters of DMAs and DMCs are highlighted in purple and green. The DMA/DMC cluster highlighted in purple is shown in detail in Fig 6.

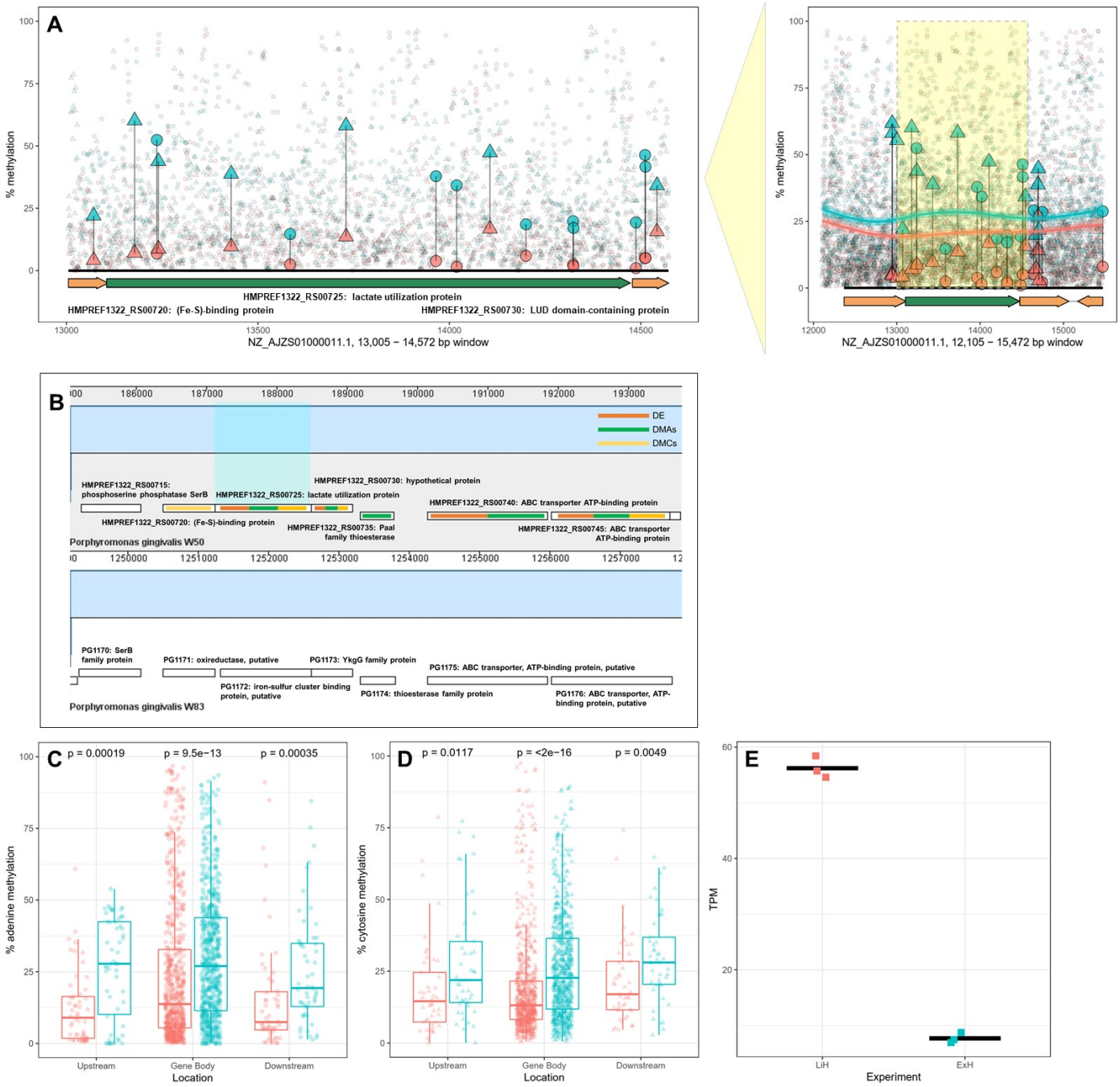

Fig 6. Genomic cluster of differential expression, adenine and cytosine methylation in the lactate utilization protein (HMPREF1322_RS00725) gene locus. Adenine (circles) and cytosine (triangles) percentage of methylation in this gene locus are shown in limited (LiH; red) and excess (ExH; blue) hemin conditions. DMAs and DMCs (larger data points) were observed within a 100 bp or 1000 bp window from the gene and a generalized additive model curve was fitted to the methylation values (A). The lactate utilization protein HMPREF1322_RS00725 was located in a cluster of genes conserved between *P. gingivalis* W50 and reference strain W83 (B). Genes in this location were affected by both DNA methylation (DMA/DMC) and gene expression (DE) changes. Differential adenine (C) and cytosine (D) methylation was statistically significant upstream (−100 bp), downstream (+100 bp) and in the gene body of HMPREF1322_RS00725 using the Wilcoxon signed-ranked test. Increased methylation in ExH was accompanied by decreased gene expression of HMPREF1322_RS00725 (E).

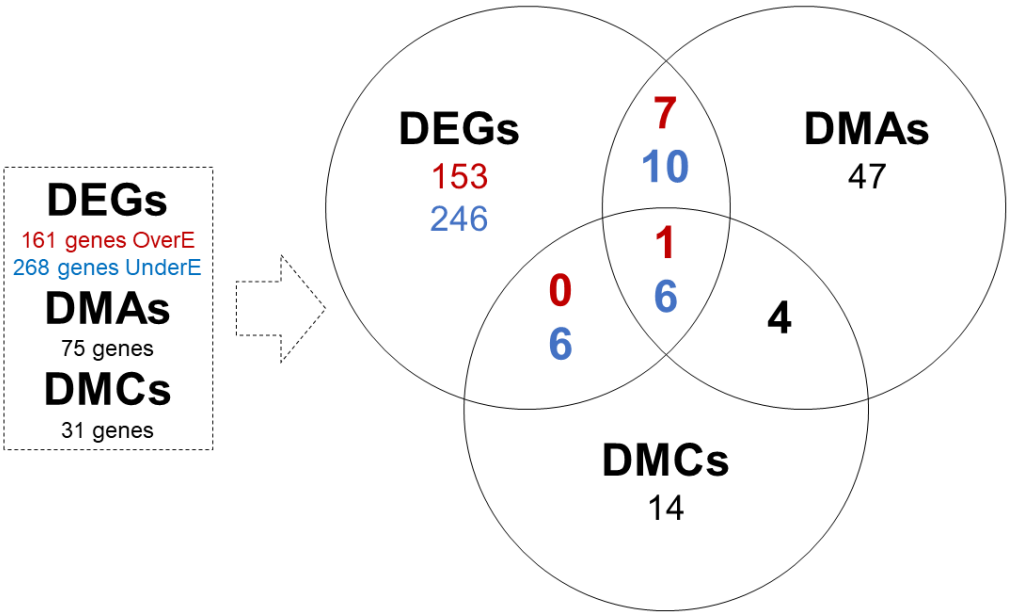

Fig 7. Overlap of genes with DEGs, DMAs and DMCs in excess hemin conditions.

Table 1. Genes most over-expressed in excess hemin conditions ordered by their significance P-value. The complete list of 161 genes is included in S1 Table.

Locus Tag	baseMean	LFC	lfcSE	P-value	Gene Symbol	Gene Product
HMPREF1322_RS04040	36595.19	3.51	0.22	5.16E-55	-	rubrerythrin family protein
HMPREF1322_RS09700	10401.67	5.11	0.38	7.99E-42	-	4Fe-4S dicluster domain-containing protein
HMPREF1322_RS02110	21476.06	5.74	0.48	4.96E-33	-	thiamine phosphate synthase
HMPREF1322_RS04875	4568.08	3.08	0.29	1.10E-26	-	RnfABCDGE type electron transport complex subunit G
HMPREF1322_RS09380	6878.27	3.42	0.34	1.63E-24	-	tRNA-Ala
HMPREF1322_RS01360	88636.17	2.13	0.21	2.51E-23	*kgp*	Lys-gingipain
HMPREF1322_RS07500	8156.19	3.17	0.32	3.27E-23	-	FtsX-like permease family protein
HMPREF1322_RS04865	8535.61	2.89	0.29	6.34E-23	*rsxC*	electron transport complex subunit RsxC
HMPREF1322_RS07540	5351.44	2.19	0.23	5.24E-22	*dnaA*	chromosomal replication initiator protein DnaA
HMPREF1322_RS01760	8591.86	2.00	0.21	2.09E-21	-	electron transfer flavoprotein subunit alpha/FixB family protein
HMPREF1322_RS02075	76668.23	2.38	0.25	7.17E-21	*rpsO*	30S ribosomal protein S15
HMPREF1322_RS07695	18257.75	2.38	0.26	1.73E-20	-	50S ribosomal protein L28
HMPREF1322_RS07305	39671.02	3.52	0.38	3.70E-20	-	SDR family oxidoreductase
HMPREF1322_RS06590	3693.30	2.34	0.26	7.00E-20	-	lipoprotein signal peptidase
HMPREF1322_RS04880	1646.03	2.96	0.33	7.77E-20	-	electron transport complex subunit E
HMPREF1322_RS07315	10873.97	2.21	0.24	2.04E-19	*pdxA*	4-hydroxythreonine-4-phosphate dehydrogenase PdxA
HMPREF1322_RS02115	802.74	3.67	0.41	3.12E-19	-	thiazole synthase
HMPREF1322_RS04430	6944.22	2.67	0.30	4.81E-19	*vorB*	3-methyl-2-oxobutanoate dehydrogenase subunit VorB
HMPREF1322_RS06505	6503.86	2.28	0.26	4.99E-19	-	succinate dehydrogenase/fumarate reductase cytochrome b subunit
HMPREF1322_RS01420	4037.78	2.32	0.27	2.55E-18	-	peptide chain release factor 2
HMPREF1322_RS06515	17162.15	1.98	0.23	4.65E-18	-	succinate dehydrogenase/fumarate reductase iron-sulfur subunit
HMPREF1322_RS06545	9763.98	2.91	0.35	5.41E-17	-	sodium ion-translocating decarboxylase subunit beta
HMPREF1322_RS07560	1584.83	1.91	0.23	6.14E-17	-	hypothetical protein
HMPREF1322_RS04870	2568.12	2.33	0.28	7.12E-17	-	RnfABCDGE type electron transport complex subunit D
HMPREF1322_RS09385	113129.22	4.77	0.57	7.41E-17	-	tRNA-Ile
HMPREF1322_RS01415	5871.99	1.89	0.23	8.89E-17	-	long-chain fatty acid--CoA ligase
HMPREF1322_RS04445	1892.04	2.05	0.25	1.71E-16	-	2-oxoglutarate ferredoxin oxidoreductase subunit gamma
HMPREF1322_RS03105	19942.29	2.37	0.29	2.99E-16	*mazG*	nucleoside triphosphate pyrophosphohydrolase
HMPREF1322_RS02105	2652.52	2.90	0.36	6.36E-16	*thiC*	phosphomethylpyrimidine synthase ThiC
HMPREF1322_RS07295	918.07	2.53	0.32	1.25E-15	-	hypothetical protein

LFC: log_2 fold change
lfcSE: Standard error of log_2 fold change

Table 2. Genes most under-expressed in excess hemin conditions (or most over-expressed in limited hemin conditions) ordered by their significance P-value. The complete list of 268 genes is included in S2 Table.

Locus Tag	baseMean	LFC	lfcSE	P-value	Gene Symbol	Gene Product
HMPREF1322_RS06000	19212.04	-7.71	0.27	1.21E-184	-	TetR/AcrR family transcriptional regulator
HMPREF1322_RS06010	7387.12	-8.06	0.28	5.34E-183	-	outer membrane lipoprotein-sorting protein
HMPREF1322_RS06015	24454.31	-7.46	0.28	2.46E-160	-	hypothetical protein
HMPREF1322_RS06005	47425.12	-7.36	0.30	1.87E-133	-	MMPL family transporter
HMPREF1322_RS05430	7754.25	-5.44	0.23	7.95E-121	-	flavodoxin
HMPREF1322_RS06790	15141.08	-6.11	0.30	3.67E-92	-	heme-binding protein HmuY
HMPREF1322_RS04145	4231.05	-5.42	0.29	7.09E-76	-	DUF4876 domain-containing protein
HMPREF1322_RS00165	33997.53	-3.86	0.24	3.60E-60	-	hypothetical protein
HMPREF1322_RS08955	18702.05	-3.75	0.23	6.92E-59	-	PglZ domain-containing protein
HMPREF1322_RS03170	5510.46	-5.17	0.32	2.13E-57	-	T9SS type A sorting domain-containing protein
HMPREF1322_RS00745	3619.54	-4.27	0.27	2.40E-57	-	ABC transporter ATP-binding protein
HMPREF1322_RS00465	1031.56	-4.52	0.29	2.04E-55	-	DUF3575 domain-containing protein
HMPREF1322_RS03855	47852.31	-3.81	0.25	8.15E-51	-	T9SS type A sorting domain-containing protein
HMPREF1322_RS05045	1138.34	-4.32	0.29	5.25E-50	-	hypothetical protein
HMPREF1322_RS07370	25172.29	-3.07	0.21	1.50E-47	-	transposase
HMPREF1322_RS05050	901.14	-3.69	0.26	5.74E-47	-	hypothetical protein
HMPREF1322_RS04140	4263.72	-5.40	0.39	9.54E-44	-	TonB-dependent receptor
HMPREF1322_RS07285	4362.71	-3.54	0.26	1.81E-42	-	IS5/IS1182 family transposase
HMPREF1322_RS00730	1091.42	-3.38	0.25	5.01E-41	-	hypothetical protein
HMPREF1322_RS10850	767.65	-3.04	0.23	6.51E-41	-	IS5/IS1182 family transposase
HMPREF1322_RS05700	1363.75	-2.92	0.22	6.42E-39	-	IS5/IS1182 family transposase
HMPREF1322_RS02830	245.42	-3.57	0.27	1.53E-38	-	helix-turn-helix domain-containing protein
HMPREF1322_RS08255	1559.13	-2.94	0.23	2.65E-38	-	IS5/IS1182 family transposase
HMPREF1322_RS00725	911.64	-2.93	0.23	5.26E-38	-	lactate utilization protein
HMPREF1322_RS05425	530.83	-3.76	0.29	1.83E-37	-	DUF2023 family protein
HMPREF1322_RS00485	425.30	-3.46	0.27	2.24E-37	-	DUF4906 domain-containing protein
HMPREF1322_RS07380	45140.22	-3.08	0.24	3.93E-37	-	family outer membrane protein
HMPREF1322_RS08605	2232.06	-4.56	0.36	4.87E-37	-	co-chaperone GroES
HMPREF1322_RS07630	1708.56	-3.97	0.31	5.27E-37	-	class I SAM-dependent methyltransferase
HMPREF1322_RS04045	1062.32	-2.77	0.22	1.27E-36	-	IS982 family transposase

LFC: log_2 fold change
lfcSE: Standard error of log_2 fold change

Table 3. DMAs (6mA) identified in *P. gingivalis* W50, selecting for a minimum mean 5% methylation difference between experimental conditions (FDR = 5% and minimum 10× coverage).

Contig	Position	Strand	mean % methylation: LiH	mean % methylation: ExH	% methylation difference	P-value	Gene ID (Locus Tag)	Gene Symbol	Gene Product	Gene on the same strand	Genes ± 1 kb away, both strands
NZ_AJZS01000047.1	40035	-	71.83%	77.08%	5.25%	7.49E-08	HMPREF1322_RS04255	*thrS*	threonine—tRNA ligase	No	HMPREF1322_RS04255
NZ_AJZS01000038.1	3559	-	4.43%	89.64%	85.21%	7.67E-08	HMPREF1322_RS03650	-	4-alpha-glucanotransferase	Yes	HMPREF1322_RS03645,HMPREF1322_RS03650
NZ_AJZS01000050.1	55602	+	53.36%	63.37%	10.01%	1.98E-07	HMPREF1322_RS04535	-	aminopeptidase	No	HMPREF1322_RS04535,HMPREF1322_RS10055
NZ_AJZS01000066.1	22242	-	15.95%	96.80%	80.86%	3.66E-07	HMPREF1322_RS06180	-	Ppx/GppA family phosphatase	Yes	HMPREF1322_RS06175,HMPREF1322_RS06180
NZ_AJZS01000011.1	13584	+	2.40%	14.66%	12.25%	5.18E-07	HMPREF1322_RS00725	-	lactate utilization protein	Yes	HMPREF1322_RS00720,HMPREF1322_RS00725, HMPREF1322_RS00730
NZ_AJZS01000009.1	24820	-	0.00%	6.32%	6.32%	1.07E-06	HMPREF1322_RS00645	*pckA*	phosphoenolpyruvate carboxykinase (ATP)	No	HMPREF1322_RS00645,HMPREF1322_RS00650, HMPREF1322_RS00655
NZ_AJZS01000097.1	917	+	6.32%	0.00%	6.32%	1.07E-06	HMPREF1322_RS09020	-	lipid A deacylase	No	HMPREF1322_RS09015,HMPREF1322_RS09020, HMPREF1322_RS09025
NZ_AJZS01000099.1	2869	-	55.68%	47.10%	8.58%	1.41E-06	-	-	-	-	HMPREF1322_RS09365,HMPREF1322_RS09370, HMPREF1322_RS09375
NZ_AJZS01000011.1	14744	+	2.00%	28.52%	26.52%	1.52E-06	HMPREF1322_RS00730	-	hypothetical protein	Yes	HMPREF1322_RS00725,HMPREF1322_RS00730, HMPREF1322_RS00735
NZ_AJZS01000020.1	1186	+	6.83%	0.00%	6.83%	1.66E-06	HMPREF1322_RS01925	-	histidinol-phosphate aminotransferase	Yes	HMPREF1322_RS01920,HMPREF1322_RS09820, HMPREF1322_RS01925
NZ_AJZS01000048.1	5988	-	0.00%	8.01%	8.01%	1.70E-06	HMPREF1322_RS10675	-	hypothetical protein	No	HMPREF1322_RS04285,HMPREF1322_RS10675, HMPREF1322_RS04295
NZ_AJZS01000011.1	14487	+	0.97%	19.32%	18.35%	2.62E-06	HMPREF1322_RS00730	-	hypothetical protein	Yes	HMPREF1322_RS00725,HMPREF1322_RS00730, HMPREF1322_RS00735
NZ_AJZS01000091.1	1018	-	16.24%	0.00%	16.24%	2.94E-06	HMPREF1322_RS08515	-	8-amino-7-oxono-noate synthase	No	HMPREF1322_RS08515
NZ_AJZS01000011.1	14511	+	4.96%	46.35%	41.39%	3.60E-06	HMPREF1322_RS00730	-	hypothetical protein	Yes	HMPREF1322_RS00725,HMPREF1322_RS00730, HMPREF1322_RS00735
NZ_AJZS01000011.1	14324	+	1.76%	17.10%	15.34%	3.75E-06	HMPREF1322_RS00725	-	lactate utilization protein	Yes	HMPREF1322_RS00725,HMPREF1322_RS00730, HMPREF1322_RS00735
NZ_AJZS01000067.1	34053	-	34.85%	21.64%	13.21%	4.13E-06	HMPREF1322_RS06415	*porQ*	type IX secretion system protein PorQ	Yes	HMPREF1322_RS06405,HMPREF1322_RS06410, HMPREF1322_RS06415
NZ_AJZS01000011.1	13965	+	3.83%	37.85%	34.02%	4.16E-06	HMPREF1322_RS00725	-	lactate utilization protein	Yes	HMPREF1322_RS00720,HMPREF1322_RS00725, HMPREF1322_RS00730
NZ_AJZS01000011.1	14644	+	5.20%	29.07%	23.87%	4.28E-06	HMPREF1322_RS00730	-	hypothetical protein	Yes	HMPREF1322_RS00725,HMPREF1322_RS00730, HMPREF1322_RS00735
NZ_AJZS01000066.1	22938	-	85.99%	37.41%	48.59%	4.56E-06	HMPREF1322_RS06180	-	Ppx/GppA family phosphatase	Yes	HMPREF1322_RS06175,HMPREF1322_RS06180, HMPREF1322_RS06185
NZ_AJZS01000038.1	3560	-	1.45%	86.22%	84.77%	5.31E-06	HMPREF1322_RS03650	-	4-alpha-glucanotransferase	Yes	HMPREF1322_RS03645,HMPREF1322_RS03650

NZ_AJZS01000011.1	13236	+	6.84%	52.42%	45.58%	5.83E-06	HMPREF1322_RS00725	-	lactate utilization protein	Yes	HMPREF1322_RS00720,HMPREF1322_RS00725
NZ_AJZS01000071.1	5863	-	62.88%	80.42%	17.54%	6.37E-06	HMPREF1322_RS07305	-	SDR family oxidoreductase	Yes	HMPREF1322_RS07300,HMPREF1322_RS07305, HMPREF1322_RS07310,HMPREF1322_RS07315
NZ_AJZS01000029.1	4423	-	5.57%	0.00%	5.57%	6.37E-06	HMPREF1322_RS03075	-	AAA domain-containing protein	Yes	HMPREF1322_RS03070,HMPREF1322_RS03075
NZ_AJZS01000046.1	4018	-	3.69%	15.60%	11.90%	6.52E-06	HMPREF1322_RS04100	-	hypothetical protein	Yes	HMPREF1322_RS04100,HMPREF1322_RS10660
NZ_AJZS01000069.1	36533	-	13.51%	18.84%	5.33%	6.81E-06	HMPREF1322_RS06610	-	ComEC/Rec2 family competence protein	No	HMPREF1322_RS06605,HMPREF1322_RS06610
NZ_AJZS01000093.1	1666	-	34.44%	16.94%	17.50%	8.21E-06	HMPREF1322_RS08685	*pruA*	L-glutamate gamma-semialdehyde dehydrogenase	Yes	HMPREF1322_RS08685,HMPREF1322_RS08690
NZ_AJZS01000011.1	14200	+	5.92%	18.54%	12.62%	8.66E-06	HMPREF1322_RS00725	-	lactate utilization protein	Yes	HMPREF1322_RS00725,HMPREF1322_RS00730, HMPREF1322_RS00735
NZ_AJZS01000063.1	3841	-	5.37%	0.00%	5.37%	8.67E-06	-	-	-	-	HMPREF1322_RS05995
NZ_AJZS01000101.1	9445	-	50.00%	75.93%	25.93%	9.71E-06	-	-	-	-	HMPREF1322_RS09650,HMPREF1322_RS09490, HMPREF1322_RS09495
NZ_AJZS01000091.1	663	-	5.19%	0.00%	5.19%	9.98E-06	HMPREF1322_RS08515	-	8-amino-7-oxono-noate synthase	No	HMPREF1322_RS08515
NZ_AJZS01000068.1	5296	-	24.60%	41.90%	17.30%	1.10E-05	HMPREF1322_RS06440	-	glycine--tRNA- ligase	Yes	HMPREF1322_RS06440,HMPREF1322_RS06445
NZ_AJZS01000011.1	15471	+	7.97%	28.75%	20.78%	1.11E-05	HMPREF1322_RS00735	-	PaaI family thioesterase	No	HMPREF1322_RS00725,HMPREF1322_RS00730, HMPREF1322_RS00735,HMPREF1322_RS00740
NZ_AJZS01000085.1	7204	-	33.33%	59.05%	25.72%	1.12E-05	HMPREF1322_RS08155	-	M56 family metallopeptidase	No	HMPREF1322_RS08150,HMPREF1322_RS08155, HMPREF1322_RS10845
NZ_AJZS01000069.1	173248	-	37.82%	19.39%	18.43%	1.14E-05	HMPREF1322_RS07250	-	site-specific integrase	No	HMPREF1322_RS07245,HMPREF1322_RS07250, HMPREF1322_RS07255
NZ_AJZS01000011.1	19392	+	7.54%	25.19%	17.66%	1.14E-05	HMPREF1322_RS00745	-	ABC transporter ATP-binding protein	No	HMPREF1322_RS00745
NZ_AJZS01000048.1	4837	-	0.00%	9.02%	9.02%	1.15E-05	-	-	-	-	HMPREF1322_RS04280,HMPREF1322_RS04285
NZ_AJZS01000011.1	17614	+	2.76%	16.42%	13.66%	1.15E-05	HMPREF1322_RS00740	-	ABC transporter ATP-binding protein	No	HMPREF1322_RS00740,HMPREF1322_RS00745
NZ_AJZS01000046.1	4605	-	6.69%	0.00%	6.69%	1.30E-05	HMPREF1322_RS10660	-	ISAs1 family transposase	Yes	HMPREF1322_RS04100,HMPREF1322_RS10660
NZ_AJZS01000001.1	12773	+	58.09%	33.33%	24.76%	1.31E-05	HMPREF1322_RS00055	-	tryptophanase	Yes	HMPREF1322_RS00055
NZ_AJZS01000025.1	6136	+	20.06%	0.00%	20.06%	1.32E-05	HMPREF1322_RS02315	-	tetratricopeptide repeat protein	No	HMPREF1322_RS02310,HMPREF1322_RS02315
NZ_AJZS01000050.1	2012	-	39.24%	1.99%	37.26%	1.46E-05	-	-	-	-	HMPREF1322_RS04325,HMPREF1322_RS04330
NZ_AJZS01000050.1	1015	+	0.00%	16.57%	16.57%	1.47E-05	HMPREF1322_RS04325	-	DUF2436 domain-containing protein	No	HMPREF1322_RS04325
NZ_AJZS01000011.1	14019	+	1.48%	34.21%	32.73%	1.48E-05	HMPREF1322_RS00725	-	lactate utilization protein	Yes	HMPREF1322_RS00720,HMPREF1322_RS00725, HMPREF1322_RS00730
NZ_AJZS01000079.1	3864	-	76.11%	60.84%	15.27%	1.52E-05	HMPREF1322_RS07770	-	DUF3298 domain-containing protein	No	HMPREF1322_RS07770,HMPREF1322_RS07775, HMPREF1322_RS07780

NZ_AJZS01000011.1	14512	+	5.03%	41.65%	36.62%	1.56E-05	HMPREF1322_RS00730	-	hypothetical protein	Yes	HMPREF1322_RS00725,HMPREF1322_RS00730, HMPREF1322_RS00735
NZ_AJZS01000007.1	2872	-	16.32%	6.02%	10.30%	1.62E-05	-	-	-	-	HMPREF1322_RS00445,HMPREF1322_RS00450
NZ_AJZS01000011.1	14323	+	2.43%	19.81%	17.38%	1.65E-05	HMPREF1322_RS00725	-	lactate utilization protein	Yes	HMPREF1322_RS00725,HMPREF1322_RS00730, HMPREF1322_RS00735
NZ_AJZS01000017.1	23369	-	13.67%	18.77%	5.10%	1.66E-05	-	-	-	-	HMPREF1322_RS01475,HMPREF1322_RS01480, HMPREF1322_RS01485,HMPREF1322_RS01490
NZ_AJZS01000021.1	7225	+	11.70%	17.64%	5.94%	1.67E-05	HMPREF1322_RS01975	-	O-acetyl-ADP-ribose deacetylase	No	HMPREF1322_RS01970,HMPREF1322_RS01975, HMPREF1322_RS01980

LiH: growth in limited hemin
ExH: growth in excess hemin

Table 4. DMCs (5mC) identified in *P. gingivalis* W50, selecting for a minimum mean 5% methylation difference between experimental conditions (FDR = 5% and minimum 10× coverage).

Contig	Position	Strand	mean % methylation: LiH	mean % methylation: ExH	% methylation difference	P-value	Gene ID (Locus Tag)	Gene Symbol	Gene Product	Gene on the same strand	Genes ± 1 kb away, both strands
NZ_AJZS01000102.1	6840	-	6.63%	12.27%	5.64%	3.39E-07	HMPREF1322_RS09535	-	pyridoxal phosphate-dependent aminotransferase	Yes	HMPREF1322_RS09535,HMPREF1322_RS09540
NZ_AJZS01000038.1	3558	-	5.53%	95.22%	89.69%	4.16E-07	HMPREF1322_RS03650	-	4-alpha-glucanotransferase	Yes	HMPREF1322_RS03645,HMPREF1322_RS03650
NZ_AJZS01000066.1	22243	-	10.21%	64.13%	53.91%	6.11E-07	HMPREF1322_RS06180	-	Ppx/GppA family phosphatase	Yes	HMPREF1322_RS06175,HMPREF1322_RS06180
NZ_AJZS01000011.1	14106	+	16.77%	47.36%	30.59%	7.45E-07	HMPREF1322_RS00725	-	lactate utilization protein	Yes	HMPREF1322_RS00720,HMPREF1322_RS00725, HMPREF1322_RS00730
NZ_AJZS01000047.1	30511	+	65.91%	58.49%	7.42%	1.42E-06	HMPREF1322_RS04210	-	S9 family peptidase	Yes	HMPREF1322_RS04205,HMPREF1322_RS04210
NZ_AJZS01000050.1	1612	-	34.96%	8.22%	26.74%	1.53E-06	HMPREF1322_RS04325	-	DUF2436 domain-containing protein	Yes	HMPREF1322_RS04325,HMPREF1322_RS04330
NZ_AJZS01000011.1	13240	+	8.76%	43.87%	35.12%	1.61E-06	HMPREF1322_RS00725	-	lactate utilization protein	Yes	HMPREF1322_RS00720,HMPREF1322_RS00725
NZ_AJZS01000011.1	12946	+	4.71%	58.08%	53.37%	2.09E-06	HMPREF1322_RS00720	-	(Fe-S)-binding protein	Yes	HMPREF1322_RS00715,HMPREF1322_RS00720, HMPREF1322_RS00725
NZ_AJZS01000011.1	13178	+	7.08%	60.16%	53.08%	2.24E-06	HMPREF1322_RS00725	-	lactate utilization protein	Yes	HMPREF1322_RS00720,HMPREF1322_RS00725
NZ_AJZS01000014.1	5938	+	34.76%	52.63%	17.87%	2.45E-06	HMPREF1322_RS00860	*htpG*	molecular chaperone HtpG	No	HMPREF1322_RS00860
NZ_AJZS01000050.1	1569	-	53.78%	2.75%	51.03%	2.69E-06	HMPREF1322_RS04325	-	DUF2436 domain-containing protein	Yes	HMPREF1322_RS04325,HMPREF1322_RS04330
NZ_AJZS01000011.1	12945	+	5.18%	61.79%	56.61%	2.71E-06	HMPREF1322_RS00720	-	(Fe-S)-binding protein	Yes	HMPREF1322_RS00715,HMPREF1322_RS00720, HMPREF1322_RS00725
NZ_AJZS01000104.1	8834	-	0.00%	7.90%	7.90%	3.17E-06	HMPREF1322_RS09610	-	tetratricopeptide repeat protein	Yes	HMPREF1322_RS09605,HMPREF1322_RS09610
NZ_AJZS01000011.1	13002	+	3.76%	55.38%	51.62%	3.63E-06	HMPREF1322_RS00720	-	(Fe-S)-binding protein	Yes	HMPREF1322_RS00715,HMPREF1322_RS00720, HMPREF1322_RS00725
NZ_AJZS01000011.1	13071	+	4.20%	21.99%	17.79%	4.48E-06	HMPREF1322_RS00720	-	(Fe-S)-binding protein	Yes	HMPREF1322_RS00720,HMPREF1322_RS00725
NZ_AJZS01000039.1	305	+	6.19%	17.19%	10.99%	4.82E-06	-	-	-	-	HMPREF1322_RS03655
NZ_AJZS01000050.1	1624	-	31.26%	11.13%	20.13%	5.57E-06	HMPREF1322_RS04325	-	DUF2436 domain-containing protein	Yes	HMPREF1322_RS04325,HMPREF1322_RS04330
NZ_AJZS01000050.1	2099	-	58.19%	8.09%	50.10%	6.00E-06	HMPREF1322_RS04330	-	nucleoside permease	Yes	HMPREF1322_RS04325,HMPREF1322_RS04330
NZ_AJZS01000037.1	41404	-	62.40%	68.48%	6.08%	6.02E-06	HMPREF1322_RS03585	-	CusA/CzcA family heavy metal efflux RND transporter	No	HMPREF1322_RS03585,HMPREF1322_RS03590
NZ_AJZS01000015.1	952	+	13.70%	22.02%	8.33%	6.03E-06	HMPREF1322_RS00885	-	U32 family peptidase	No	HMPREF1322_RS00880,HMPREF1322_RS00885

NZ_AJZS01000050.1	1920	-	64.72%	8.39%	56.32%	7.23E-06	-	-	-	-	HMPREF1322_RS04325,HMPREF1322_RS04330
NZ_AJZS01000011.1	14698	+	26.82%	44.78%	17.96%	7.90E-06	HMPREF1322_RS00730	-	hypothetical protein	Yes	HMPREF1322_RS00725,HMPREF1322_RS00730, HMPREF1322_RS00735
NZ_AJZS01000046.1	1044	-	10.78%	5.27%	5.52%	8.29E-06	HMPREF1322_RS04090	-	MBOAT family protein	Yes	HMPREF1322_RS04090,HMPREF1322_RS04095
NZ_AJZS01000011.1	14542	+	15.67%	34.20%	18.53%	8.76E-06	HMPREF1322_RS00730	-	hypothetical protein	Yes	HMPREF1322_RS00725,HMPREF1322_RS00730, HMPREF1322_RS00735
NZ_AJZS01000041.1	4471	-	17.52%	22.93%	5.41%	9.62E-06	-	-	-	-	HMPREF1322_RS03860,HMPREF1322_RS03870, HMPREF1322_RS03875
NZ_AJZS01000050.1	1625	-	26.00%	9.52%	16.48%	9.79E-06	HMPREF1322_RS04325	-	DUF2436 domain-containing protein	Yes	HMPREF1322_RS04325,HMPREF1322_RS04330
NZ_AJZS01000015.1	78713	-	64.82%	58.15%	6.67%	1.08E-05	HMPREF1322_RS01240	-	iron ABC transporter permease	Yes	HMPREF1322_RS01240,HMPREF1322_RS01245
NZ_AJZS01000011.1	13730	+	13.59%	58.15%	44.56%	1.13E-05	HMPREF1322_RS00725	-	lactate utilization protein	Yes	HMPREF1322_RS00720,HMPREF1322_RS00725, HMPREF1322_RS00730
NZ_AJZS01000050.1	2262	-	53.40%	9.81%	43.59%	1.20E-05	HMPREF1322_RS04330	-	nucleoside permease	Yes	HMPREF1322_RS04325,HMPREF1322_RS04330
NZ_AJZS01000011.1	14669	+	7.23%	19.84%	12.61%	1.28E-05	HMPREF1322_RS00730	-	hypothetical protein	Yes	HMPREF1322_RS00725,HMPREF1322_RS00730, HMPREF1322_RS00735
NZ_AJZS01000089.1	26	+	0.00%	9.03%	9.03%	1.34E-05	HMPREF1322_RS08455	-	IS5/IS1182 family transposase	Yes	HMPREF1322_RS08455,HMPREF1322_RS08460
NZ_AJZS01000011.1	14706	+	2.91%	21.70%	18.79%	1.52E-05	HMPREF1322_RS00730	-	hypothetical protein	Yes	HMPREF1322_RS00725,HMPREF1322_RS00730, HMPREF1322_RS00735
NZ_AJZS01000050.1	2002	-	58.99%	4.81%	54.18%	1.57E-05	-	-	-	-	HMPREF1322_RS04325,HMPREF1322_RS04330
NZ_AJZS01000036.1	5418	+	22.76%	14.46%	8.30%	1.59E-05	HMPREF1322_RS03420	-	YjgP/YjgQ family permease	No	HMPREF1322_RS03410,HMPREF1322_RS03415, HMPREF1322_RS03420,HMPREF1322_RS03425
NZ_AJZS01000050.1	2101	-	53.34%	4.65%	48.69%	1.74E-05	HMPREF1322_RS04330	-	nucleoside permease	Yes	HMPREF1322_RS04325,HMPREF1322_RS04330
NZ_AJZS01000080.1	123	+	12.46%	0.00%	12.46%	1.76E-05	HMPREF1322_RS07835	-	hypothetical protein	Yes	HMPREF1322_RS07835,HMPREF1322_RS07840, HMPREF1322_RS07845
NZ_AJZS01000080.1	124	+	12.46%	0.00%	12.46%	1.76E-05	HMPREF1322_RS07835	-	hypothetical protein	Yes	HMPREF1322_RS07835,HMPREF1322_RS07840, HMPREF1322_RS07845
NZ_AJZS01000011.1	14693	+	14.07%	38.73%	24.67%	1.77E-05	HMPREF1322_RS00730	-	hypothetical protein	Yes	HMPREF1322_RS00725,HMPREF1322_RS00730, HMPREF1322_RS00735
NZ_AJZS01000069.1	3434	-	51.80%	41.48%	10.32%	1.97E-05	HMPREF1322_RS06465	-	hypothetical protein	Yes	HMPREF1322_RS06460,HMPREF1322_RS06465, HMPREF1322_RS06470
NZ_AJZS01000013.1	2448	-	11.90%	17.41%	5.51%	2.20E-05	HMPREF1322_RS00790	*gyrA*	DNA gyrase subunit A	Yes	HMPREF1322_RS00785,HMPREF1322_RS00790
NZ_AJZS01000050.1	1769	-	49.12%	2.56%	46.56%	2.20E-05	-	-	-	-	HMPREF1322_RS04325,HMPREF1322_RS04330
NZ_AJZS01000066.1	22943	+	70.43%	31.90%	38.53%	2.21E-05	HMPREF1322_RS06180	-	Ppx/GppA family phosphatase	No	HMPREF1322_RS06175,HMPREF1322_RS06180, HMPREF1322_RS06185
NZ_AJZS01000050.1	797	-	38.96%	13.79%	25.16%	2.31E-05	HMPREF1322_RS04325	-	DUF2436 domain-containing protein	Yes	HMPREF1322_RS04325
NZ_AJZS01000011.1	18653	+	4.65%	18.69%	14.04%	2.34E-05	HMPREF1322_RS00745	-	ABC transporter ATP-binding protein	No	HMPREF1322_RS00740,HMPREF1322_RS00745

NZ_AJZS01000009.1	3668	+	12.68%	21.61%	8.93%	2.40E-05	HMPREF1322_RS00555	-	DEAD/DEAH box helicase family protein	No	HMPREF1322_RS00555,HMPREF1322_RS00560
NZ_AJZS01000011.1	13430	+	9.65%	38.76%	29.11%	2.55E-05	HMPREF1322_RS00725	-	lactate utilization protein	Yes	HMPREF1322_RS00720,HMPREF1322_RS00725
NZ_AJZS01000050.1	2103	-	61.60%	6.56%	55.04%	2.66E-05	HMPREF1322_RS04330	-	nucleoside permease	Yes	HMPREF1322_RS04325,HMPREF1322_RS04330

LiH: growth in limited hemin
ExH: growth in excess hemin

Table 5. Genes over-expressed in excess hemin conditions with DMAs (> 1.5 LFC, > 5% methylation difference, FDR = 5%).

Locus Tag	Gene Symbol	Gene Product	Contig	Gene start	Gene end	Strand Expr.	Methylated Position	Strand Meth.	Distance Meth.	DE analysis			DM analysis			
										baseMean	LFC	P-value	mean % methylation: LiH	mean % methylation: ExH	% methylation difference	P-value
HMPREF1322_RS07305	-	SDR family oxidoreductase	NZ_AJZS01000071.1	5169	5900	-	5863	-	694	39671.02	3.52	3.70E-20	62.88%	80.42%	17.54%	6.37E-06
HMPREF1322_RS07315	*pdxA*	4-hydroxythreonine-4-phosphate dehydrogenase PdxA	NZ_AJZS01000071.1	6386	7483	-	5863	-	-523	10873.97	2.21	2.04E-19	62.88%	80.42%	17.54%	6.37E-06
HMPREF1322_RS06180	-	Ppx/GppA family phosphatase	NZ_AJZS01000066.1	22201	23108	-	22242	-	41	914.83	1.59	2.19E-12	15.95%	96.80%	80.86%	3.66E-07
HMPREF1322_RS06180	-	Ppx/GppA family phosphatase	NZ_AJZS01000066.1	22201	23108	-	22938	-	737	914.83	1.59	2.19E-12	85.99%	37.41%	48.59%	4.56E-06
HMPREF1322_RS01480	-	tRNA-Thr	NZ_AJZS01000017.1	23424	23496	-	23369	-	-55	362.80	2.29	2.35E-12	13.67%	18.77%	5.10%	1.66E-05
HMPREF1322_RS01485	-	hypothetical protein	NZ_AJZS01000017.1	23557	24009	-	23369	-	-188	2236.75	2.55	9.57E-12	13.67%	18.77%	5.10%	1.66E-05
HMPREF1322_RS04280	*dnaE*	DNA polymerase III subunit alpha	NZ_AJZS01000048.1	883	4569	-	4837	-	3954	4976.97	1.52	1.59E-09	0.00%	9.02%	9.02%	1.15E-05
HMPREF1322_RS04100	-	hypothetical protein	NZ_AJZS01000046.1	2632	4023	-	4018	-	1386	3442.27	1.59	9.47E-09	3.69%	15.60%	11.90%	6.52E-06
HMPREF1322_RS04100	-	hypothetical protein	NZ_AJZS01000046.1	2632	4023	-	4605	-	1973	3442.27	1.59	9.47E-09	6.69%	0.00%	6.69%	1.30E-05
HMPREF1322_RS09370	*rrf*	5S ribosomal RNA	NZ_AJZS01000099.1	3390	3500	-	2869	-	-521	5793.67	1.71	6.69E-04	55.68%	47.10%	8.58%	1.41E-06

Strand Expr: Strand of the gene
Strand Meth: Strand of the methylated position
Distance Meth: Distance of the methylated position to the gene start site in base pairs, negative values indicate upstream location
DE analysis: results from the differential expression analysis
DM analysis: results from the differential methylation analysis
LFC: log_2 fold change
LiH: growth in limited hemin
ExH: growth in excess hemin

Table 6. Genes under-expressed in excess hemin conditions with DMAs (< -1.5 LFC, > 5% methylation difference, FDR = 5%).

Locus Tag	Gene Symbol	Gene Product	Contig	Gene start	Gene end	Strand Expr.	Methylated Position	Strand Meth.	Distance Meth.	DE analysis			DM analysis			
										baseMean	LFC	P-value	mean % methylation: LiH	mean % methylation: ExH	% methylation difference	P-value
HMPREF1322_RS00745	-	ABC transporter ATP-binding protein	NZ_AJZS01000011.1	17886	19607	-	17614	+	-272	3619.54	-4.27	2.40E-57	2.76%	16.42%	13.66%	1.15E-05
HMPREF1322_RS00745	-	ABC transporter ATP-binding protein	NZ_AJZS01000011.1	17886	19607	-	19392	+	1506	3619.54	-4.27	2.40E-57	7.54%	25.19%	17.66%	1.14E-05
HMPREF1322_RS00730	-	hypothetical protein	NZ_AJZS01000011.1	14478	15062	+	13584	+	-894	1091.42	-3.38	5.01E-41	2.40%	14.66%	12.25%	5.18E-07
HMPREF1322_RS00730	-	hypothetical protein	NZ_AJZS01000011.1	14478	15062	+	13965	+	-513	1091.42	-3.38	5.01E-41	3.83%	37.85%	34.02%	4.16E-06
HMPREF1322_RS00730	-	hypothetical protein	NZ_AJZS01000011.1	14478	15062	+	14019	+	-459	1091.42	-3.38	5.01E-41	1.48%	34.21%	32.73%	1.48E-05
HMPREF1322_RS00730	-	hypothetical protein	NZ_AJZS01000011.1	14478	15062	+	14200	+	-278	1091.42	-3.38	5.01E-41	5.92%	18.54%	12.62%	8.66E-06
HMPREF1322_RS00730	-	hypothetical protein	NZ_AJZS01000011.1	14478	15062	+	14323	+	-155	1091.42	-3.38	5.01E-41	2.43%	19.81%	17.38%	1.65E-05
HMPREF1322_RS00730	-	hypothetical protein	NZ_AJZS01000011.1	14478	15062	+	14324	+	-154	1091.42	-3.38	5.01E-41	1.76%	17.10%	15.34%	3.75E-06
HMPREF1322_RS00730	-	hypothetical protein	NZ_AJZS01000011.1	14478	15062	+	14487	+	9	1091.42	-3.38	5.01E-41	0.97%	19.32%	18.35%	2.62E-06
HMPREF1322_RS00730	-	hypothetical protein	NZ_AJZS01000011.1	14478	15062	+	14511	+	33	1091.42	-3.38	5.01E-41	4.96%	46.35%	41.39%	3.60E-06
HMPREF1322_RS00730	-	hypothetical protein	NZ_AJZS01000011.1	14478	15062	+	14512	+	34	1091.42	-3.38	5.01E-41	5.03%	41.65%	36.62%	1.56E-05
HMPREF1322_RS00730	-	hypothetical protein	NZ_AJZS01000011.1	14478	15062	+	14644	+	166	1091.42	-3.38	5.01E-41	5.20%	29.07%	23.87%	4.28E-06
HMPREF1322_RS00730	-	hypothetical protein	NZ_AJZS01000011.1	14478	15062	+	14744	+	266	1091.42	-3.38	5.01E-41	2.00%	28.52%	26.52%	1.52E-06
HMPREF1322_RS00730	-	hypothetical protein	NZ_AJZS01000011.1	14478	15062	+	15471	+	993	1091.42	-3.38	5.01E-41	7.97%	28.75%	20.78%	1.11E-05
HMPREF1322_RS00725	-	lactate utilization protein	NZ_AJZS01000011.1	13105	14472	+	13236	+	131	911.64	-2.93	5.26E-38	6.84%	52.42%	45.58%	5.83E-06
HMPREF1322_RS00725	-	lactate utilization protein	NZ_AJZS01000011.1	13105	14472	+	13584	+	479	911.64	-2.93	5.26E-38	2.40%	14.66%	12.25%	5.18E-07
HMPREF1322_RS00725	-	lactate utilization protein	NZ_AJZS01000011.1	13105	14472	+	13965	+	860	911.64	-2.93	5.26E-38	3.83%	37.85%	34.02%	4.16E-06
HMPREF1322_RS00725	-	lactate utilization protein	NZ_AJZS01000011.1	13105	14472	+	14019	+	914	911.64	-2.93	5.26E-38	1.48%	34.21%	32.73%	1.48E-05
HMPREF1322_RS00725	-	lactate utilization protein	NZ_AJZS01000011.1	13105	14472	+	14200	+	1095	911.64	-2.93	5.26E-38	5.92%	18.54%	12.62%	8.66E-06

HMPREF1322_RS00725	-	lactate utilization protein	NZ_AJZS01000011.1	13105	14472	+	14323	+	1218	911.64	-2.93	5.26E-38	2.43%	19.81%	17.38%	1.65E-05
HMPREF1322_RS00725	-	lactate utilization protein	NZ_AJZS01000011.1	13105	14472	+	14324	+	1219	911.64	-2.93	5.26E-38	1.76%	17.10%	15.34%	3.75E-06
HMPREF1322_RS00725	-	lactate utilization protein	NZ_AJZS01000011.1	13105	14472	+	14487	+	1382	911.64	-2.93	5.26E-38	0.97%	19.32%	18.35%	2.62E-06
HMPREF1322_RS00725	-	lactate utilization protein	NZ_AJZS01000011.1	13105	14472	+	14511	+	1406	911.64	-2.93	5.26E-38	4.96%	46.35%	41.39%	3.60E-06
HMPREF1322_RS00725	-	lactate utilization protein	NZ_AJZS01000011.1	13105	14472	+	14512	+	1407	911.64	-2.93	5.26E-38	5.03%	41.65%	36.62%	1.56E-05
HMPREF1322_RS00725	-	lactate utilization protein	NZ_AJZS01000011.1	13105	14472	+	14644	+	1539	911.64	-2.93	5.26E-38	5.20%	29.07%	23.87%	4.28E-06
HMPREF1322_RS00725	-	lactate utilization protein	NZ_AJZS01000011.1	13105	14472	+	14744	+	1639	911.64	-2.93	5.26E-38	2.00%	28.52%	26.52%	1.52E-06
HMPREF1322_RS00725	-	lactate utilization protein	NZ_AJZS01000011.1	13105	14472	+	15471	+	2366	911.64	-2.93	5.26E-38	7.97%	28.75%	20.78%	1.11E-05
HMPREF1322_RS01975	-	O-acetyl-ADP-ribose deacetylase	NZ_AJZS01000021.1	7184	7678	-	7225	+	41	6623.03	-2.30	2.87E-18	11.70%	17.64%	5.94%	1.67E-05
HMPREF1322_RS02315	-	tetratricopeptide repeat protein	NZ_AJZS01000025.1	5372	7181	-	6136	+	764	11707.30	-3.03	4.40E-17	20.06%	0.00%	20.06%	1.32E-05
HMPREF1322_RS03650	-	4-alpha-glucanotransferase	NZ_AJZS01000038.1	2961	4847	-	3559	-	598	5951.70	-2.22	5.69E-14	4.43%	89.64%	85.21%	7.67E-08
HMPREF1322_RS03650	-	4-alpha-glucanotransferase	NZ_AJZS01000038.1	2961	4847	-	3560	-	599	5951.70	-2.22	5.69E-14	1.45%	86.22%	84.77%	5.31E-06
HMPREF1322_RS02310	-	response regulator transcription factor	NZ_AJZS01000025.1	4676	5359	-	6136	+	1460	10536.03	-1.99	1.34E-13	20.06%	0.00%	20.06%	1.32E-05
HMPREF1322_RS01980	-	UDP-2,3-diacylglucosamine diphosphatase	NZ_AJZS01000021.1	7760	8548	-	7225	+	-535	13336.64	-1.78	2.46E-13	11.70%	17.64%	5.94%	1.67E-05
HMPREF1322_RS07250	-	site-specific integrase	NZ_AJZS01000069.1	173000	174202	+	173248	-	248	320.75	-1.58	8.34E-11	37.82%	19.39%	18.43%	1.14E-05
HMPREF1322_RS00740	-	ABC transporter ATP-binding protein	NZ_AJZS01000011.1	16133	17839	-	15471	+	-662	7059.72	-2.68	5.06E-10	7.97%	28.75%	20.78%	1.11E-05
HMPREF1322_RS00740	-	ABC transporter ATP-binding protein	NZ_AJZS01000011.1	16133	17839	-	17614	+	1481	7059.72	-2.68	5.06E-10	2.76%	16.42%	13.66%	1.15E-05
HMPREF1322_RS09495	-	hypothetical protein	NZ_AJZS01000101.1	10189	10749	+	9445	-	-744	6645.00	-2.53	3.50E-09	50.00%	75.93%	25.93%	9.71E-06
HMPREF1322_RS07780	-	MBL fold metallo-hydrolase	NZ_AJZS01000079.1	4600	5244	+	3864	-	-736	2319.58	-2.32	2.51E-06	76.11%	60.84%	15.27%	1.52E-05
HMPREF1322_RS08150	-	BlaI/MecI/CopY family transcriptional regulator	NZ_AJZS01000085.1	6031	6411	+	7204	-	1173	403.18	-1.74	2.90E-06	33.33%	59.05%	25.72%	1.12E-05

HMPREF1322_RS10055	-	hypothetical protein	NZ_AJZS01000050.1	56011	56172	+	55602	+	-409	18.27	-1.91	7.10E-04	53.36%	63.37%	10.01%	1.98E-07
HMPREF1322_RS09820	-	hypothetical protein	NZ_AJZS01000020.1	830	1045	+	1186	+	356	251.64	-1.72	1.04E-03	6.83%	0.00%	6.83%	1.66E-06

Strand Expr: Strand of the gene
Strand Meth: Strand of the methylated position
Distance Meth: Distance of the methylated position to the gene start site in base pairs, negative values indicate upstream location
DE analysis: results from the differential expression analysis
DM analysis: results from the differential methylation analysis
LFC: log_2 fold change
LiH: growth in limited hemin
ExH: growth in excess hemin

Table 7. Genes over-expressed in excess hemin conditions with DMCs (> 1.5 LFC, > 5% methylation difference, FDR = 5%).

Locus Tag	Gene Symbol	Gene Product	Contig	Gene start	Gene end	Strand Expr.	Methylated Position	Strand Meth.	Distance Meth.	DE analysis			DM analysis			
										baseMean	LFC	P-value	mean % methylation: LiH	mean % methylation: ExH	% methylation difference	P-value
HMPREF1322_RS06180	-	Ppx/GppA family phosphatase	NZ_AJZS01000066.1	22201	23108	-	22243	-	42	914.83	1.59	2.19E-12	10.21%	64.13%	53.91%	6.11E-07
HMPREF1322_RS06180	-	Ppx/GppA family phosphatase	NZ_AJZS01000066.1	22201	23108	-	22943	+	742	914.83	1.59	2.19E-12	70.43%	31.90%	38.53%	2.21E-05

Strand Expr: Strand of the gene
Strand Meth: Strand of the methylated position
Distance Meth: Distance of the methylated position to the gene start site in base pairs, negative values indicate upstream location
DE analysis: results from the differential expression analysis
DM analysis: results from the differential methylation analysis
LFC: log_2 fold change
LiH: growth in limited hemin
ExH: growth in excess hemin

Table 8. Genes under-expressed in excess hemin conditions with DMCs (< -1.5 LFC, > 5% methylation difference, FDR = 5%).

Locus Tag	Gene Symbol	Gene Product	Contig	Gene start	Gene end	Strand Expr.	Methylated Position	Strand Meth.	Distance Meth.	DE analysis			DM analysis			
										baseMean	LFC	P-value	mean % methylation: LiH	mean % methylation: ExH	% methylation difference	P-value
HMPREF1322_RS00745	-	ABC transporter ATP-binding protein	NZ_AJZS01000011.1	17886	19607	-	18653	+	767	3619.54	-4.27	2.40E-57	4.65%	18.69%	14.04%	2.34E-05
HMPREF1322_RS00730	-	hypothetical protein	NZ_AJZS01000011.1	14478	15062	+	13730	+	-748	1091.42	-3.38	5.01E-41	13.59%	58.15%	44.56%	1.13E-05
HMPREF1322_RS00730	-	hypothetical protein	NZ_AJZS01000011.1	14478	15062	+	14106	+	-372	1091.42	-3.38	5.01E-41	16.77%	47.36%	30.59%	7.45E-07
HMPREF1322_RS00730	-	hypothetical protein	NZ_AJZS01000011.1	14478	15062	+	14542	+	64	1091.42	-3.38	5.01E-41	15.67%	34.20%	18.53%	8.76E-06
HMPREF1322_RS00730	-	hypothetical protein	NZ_AJZS01000011.1	14478	15062	+	14669	+	191	1091.42	-3.38	5.01E-41	7.23%	19.84%	12.61%	1.28E-05
HMPREF1322_RS00730	-	hypothetical protein	NZ_AJZS01000011.1	14478	15062	+	14693	+	215	1091.42	-3.38	5.01E-41	14.07%	38.73%	24.67%	1.77E-05
HMPREF1322_RS00730	-	hypothetical protein	NZ_AJZS01000011.1	14478	15062	+	14698	+	220	1091.42	-3.38	5.01E-41	26.82%	44.78%	17.96%	7.90E-06
HMPREF1322_RS00730	-	hypothetical protein	NZ_AJZS01000011.1	14478	15062	+	14706	+	228	1091.42	-3.38	5.01E-41	2.91%	21.70%	18.79%	1.52E-05
HMPREF1322_RS00725	-	lactate utilization protein	NZ_AJZS01000011.1	13105	14472	+	12945	+	-160	911.64	-2.93	5.26E-38	5.18%	61.79%	56.61%	2.71E-06
HMPREF1322_RS00725	-	lactate utilization protein	NZ_AJZS01000011.1	13105	14472	+	12946	+	-159	911.64	-2.93	5.26E-38	4.71%	58.08%	53.37%	2.09E-06
HMPREF1322_RS00725	-	lactate utilization protein	NZ_AJZS01000011.1	13105	14472	+	13002	+	-103	911.64	-2.93	5.26E-38	3.76%	55.38%	51.62%	3.63E-06
HMPREF1322_RS00725	-	lactate utilization protein	NZ_AJZS01000011.1	13105	14472	+	13071	+	-34	911.64	-2.93	5.26E-38	4.20%	21.99%	17.79%	4.48E-06
HMPREF1322_RS00725	-	lactate utilization protein	NZ_AJZS01000011.1	13105	14472	+	13178	+	73	911.64	-2.93	5.26E-38	7.08%	60.16%	53.08%	2.24E-06
HMPREF1322_RS00725	-	lactate utilization protein	NZ_AJZS01000011.1	13105	14472	+	13240	+	135	911.64	-2.93	5.26E-38	8.76%	43.87%	35.12%	1.61E-06
HMPREF1322_RS00725	-	lactate utilization protein	NZ_AJZS01000011.1	13105	14472	+	13430	+	325	911.64	-2.93	5.26E-38	9.65%	38.76%	29.11%	2.55E-05
HMPREF1322_RS00725	-	lactate utilization protein	NZ_AJZS01000011.1	13105	14472	+	13730	+	625	911.64	-2.93	5.26E-38	13.59%	58.15%	44.56%	1.13E-05
HMPREF1322_RS00725	-	lactate utilization protein	NZ_AJZS01000011.1	13105	14472	+	14106	+	1001	911.64	-2.93	5.26E-38	16.77%	47.36%	30.59%	7.45E-07
HMPREF1322_RS00725	-	lactate utilization protein	NZ_AJZS01000011.1	13105	14472	+	14542	+	1437	911.64	-2.93	5.26E-38	15.67%	34.20%	18.53%	8.76E-06
HMPREF1322_RS00725	-	lactate utilization protein	NZ_AJZS01000011.1	13105	14472	+	14669	+	1564	911.64	-2.93	5.26E-38	7.23%	19.84%	12.61%	1.28E-05

HMPREF1322_RS00725	-	lactate utilization protein	NZ_AJZS01000011.1	13105	14472	+	14693	+	1588	911.64	-2.93	5.26E-38	14.07%	38.73%	24.67%	1.77E-05
HMPREF1322_RS00725	-	lactate utilization protein	NZ_AJZS01000011.1	13105	14472	+	14698	+	1593	911.64	-2.93	5.26E-38	26.82%	44.78%	17.96%	7.90E-06
HMPREF1322_RS00725	-	lactate utilization protein	NZ_AJZS01000011.1	13105	14472	+	14706	+	1601	911.64	-2.93	5.26E-38	2.91%	21.70%	18.79%	1.52E-05
HMPREF1322_RS00885	-	U32 family peptidase	NZ_AJZS01000015.1	486	2393	-	952	+	466	3114.91	-3.09	3.14E-27	13.70%	22.02%	8.33%	6.03E-06
HMPREF1322_RS00860	*htpG*	molecular chaperone HtpG	NZ_AJZS01000014.1	5016	7070	-	5938	+	922	15163.58	-2.87	2.96E-23	34.76%	52.63%	17.87%	2.45E-06
HMPREF1322_RS06465	-	hypothetical protein	NZ_AJZS01000069.1	2552	3754	-	3434	-	882	153316.28	-2.35	1.18E-19	51.80%	41.48%	10.32%	1.97E-05
HMPREF1322_RS03650	-	4-alpha-glucanotransferase	NZ_AJZS01000038.1	2961	4847	-	3558	-	597	5951.70	-2.22	5.69E-14	5.53%	95.22%	89.69%	4.16E-07
HMPREF1322_RS06460	-	transporter	NZ_AJZS01000069.1	784	2448	-	3434	-	2650	37619.48	-2.01	1.02E-13	51.80%	41.48%	10.32%	1.97E-05
HMPREF1322_RS00740	-	ABC transporter ATP-binding protein	NZ_AJZS01000011.1	16133	17839	-	18653	+	2520	7059.72	-2.68	5.06E-10	4.65%	18.69%	14.04%	2.34E-05
HMPREF1322_RS03860	-	histidinol phosphate phosphatase	NZ_AJZS01000041.1	3824	4342	-	4471	-	647	15144.78	-1.52	1.09E-09	17.52%	22.93%	5.41%	9.62E-06
HMPREF1322_RS00880	-	DUF1661 domain-containing protein	NZ_AJZS01000015.1	1	203	-	952	+	951	129.52	-1.93	8.19E-07	13.70%	22.02%	8.33%	6.03E-06

Strand Expr: Strand of the gene
Strand Meth: Strand of the methylated position
Distance Meth: Distance of the methylated position to the gene start site in base pairs, negative values indicate upstream location
DE analysis: results from the differential expression analysis
DM analysis: results from the differential methylation analysis
LFC: log_2 fold change
LiH: growth in limited hemin
ExH: growth in excess hemin

Table 9. Differentially expressed genes with DMAs and DMCs in excess hemin conditions (< -1.5 LFC, > 5% methylation difference, FDR = 5%).

Locus Tag	Gene Symbol	Gene Product	Contig	Gene start	Gene end	Strand Expr.	Methylated Position	Strand Meth.	Distance Meth.	DE analysis				DM analysis				
										Direction	baseMean	LFC	P-value	Modification	mean % methylation: LiH	mean % methylation: ExH	% methylation difference	P-value
HMPREF1322_RS00725	-	lactate utilization protein	NZ_AJZS01000011.1	13105	14472	+	12945	+	-160	Under expr.	911.64	-2.93	5.26E-38	DMC	5.18%	61.79%	56.61%	2.71E-06
HMPREF1322_RS00725	-	lactate utilization protein	NZ_AJZS01000011.1	13105	14472	+	12946	+	-159	Under expr.	911.64	-2.93	5.26E-38	DMC	4.71%	58.08%	53.37%	2.09E-06
HMPREF1322_RS00725	-	lactate utilization protein	NZ_AJZS01000011.1	13105	14472	+	13002	+	-103	Under expr.	911.64	-2.93	5.26E-38	DMC	3.76%	55.38%	51.62%	3.63E-06
HMPREF1322_RS00725	-	lactate utilization protein	NZ_AJZS01000011.1	13105	14472	+	13071	+	-34	Under expr.	911.64	-2.93	5.26E-38	DMC	4.20%	21.99%	17.79%	4.48E-06
HMPREF1322_RS00725	-	lactate utilization protein	NZ_AJZS01000011.1	13105	14472	+	13178	+	73	Under expr.	911.64	-2.93	5.26E-38	DMC	7.08%	60.16%	53.08%	2.24E-06
HMPREF1322_RS00725	-	lactate utilization protein	NZ_AJZS01000011.1	13105	14472	+	13236	+	131	Under expr.	911.64	-2.93	5.26E-38	DMA	6.84%	52.42%	45.58%	5.83E-06
HMPREF1322_RS00725	-	lactate utilization protein	NZ_AJZS01000011.1	13105	14472	+	13240	+	135	Under expr.	911.64	-2.93	5.26E-38	DMC	8.76%	43.87%	35.12%	1.61E-06
HMPREF1322_RS00725	-	lactate utilization protein	NZ_AJZS01000011.1	13105	14472	+	13430	+	325	Under expr.	911.64	-2.93	5.26E-38	DMC	9.65%	38.76%	29.11%	2.55E-05
HMPREF1322_RS00725	-	lactate utilization protein	NZ_AJZS01000011.1	13105	14472	+	13584	+	479	Under expr.	911.64	-2.93	5.26E-38	DMA	2.40%	14.66%	12.25%	5.18E-07
HMPREF1322_RS00725	-	lactate utilization protein	NZ_AJZS01000011.1	13105	14472	+	13730	+	625	Under expr.	911.64	-2.93	5.26E-38	DMC	13.59%	58.15%	44.56%	1.13E-05
HMPREF1322_RS00725	-	lactate utilization protein	NZ_AJZS01000011.1	13105	14472	+	13965	+	860	Under expr.	911.64	-2.93	5.26E-38	DMA	3.83%	37.85%	34.02%	4.16E-06
HMPREF1322_RS00725	-	lactate utilization protein	NZ_AJZS01000011.1	13105	14472	+	14019	+	914	Under expr.	911.64	-2.93	5.26E-38	DMA	1.48%	34.21%	32.73%	1.48E-05
HMPREF1322_RS00725	-	lactate utilization protein	NZ_AJZS01000011.1	13105	14472	+	14106	+	1001	Under expr.	911.64	-2.93	5.26E-38	DMC	16.77%	47.36%	30.59%	7.45E-07
HMPREF1322_RS00725	-	lactate utilization protein	NZ_AJZS01000011.1	13105	14472	+	14200	+	1095	Under expr.	911.64	-2.93	5.26E-38	DMA	5.92%	18.54%	12.62%	8.66E-06
HMPREF1322_RS00725	-	lactate utilization protein	NZ_AJZS01000011.1	13105	14472	+	14323	+	1218	Under expr.	911.64	-2.93	5.26E-38	DMA	2.43%	19.81%	17.38%	1.65E-05
HMPREF1322_RS00725	-	lactate utilization protein	NZ_AJZS01000011.1	13105	14472	+	14324	+	1219	Under expr.	911.64	-2.93	5.26E-38	DMA	1.76%	17.10%	15.34%	3.75E-06
HMPREF1322_RS00725	-	lactate utilization protein	NZ_AJZS01000011.1	13105	14472	+	14487	+	1382	Under expr.	911.64	-2.93	5.26E-38	DMA	0.97%	19.32%	18.35%	2.62E-06
HMPREF1322_RS00725	-	lactate utilization protein	NZ_AJZS01000011.1	13105	14472	+	14511	+	1406	Under expr.	911.64	-2.93	5.26E-38	DMA	4.96%	46.35%	41.39%	3.60E-06
HMPREF1322_RS00725	-	lactate utilization protein	NZ_AJZS01000011.1	13105	14472	+	14512	+	1407	Under expr.	911.64	-2.93	5.26E-38	DMA	5.03%	41.65%	36.62%	1.56E-05
HMPREF1322_RS00725	-	lactate utilization protein	NZ_AJZS01000011.1	13105	14472	+	14542	+	1437	Under expr.	911.64	-2.93	5.26E-38	DMC	15.67%	34.20%	18.53%	8.76E-06
HMPREF1322_RS00725	-	lactate utilization protein	NZ_AJZS01000011.1	13105	14472	+	14644	+	1539	Under expr.	911.64	-2.93	5.26E-38	DMA	5.20%	29.07%	23.87%	4.28E-06
HMPREF1322_RS00725	-	lactate utilization protein	NZ_AJZS01000011.1	13105	14472	+	14669	+	1564	Under expr.	911.64	-2.93	5.26E-38	DMC	7.23%	19.84%	12.61%	1.28E-05
HMPREF1322_RS00725	-	lactate utilization protein	NZ_AJZS01000011.1	13105	14472	+	14693	+	1588	Under expr.	911.64	-2.93	5.26E-38	DMC	14.07%	38.73%	24.67%	1.77E-05
HMPREF1322_RS00725	-	lactate utilization protein	NZ_AJZS01000011.1	13105	14472	+	14698	+	1593	Under expr.	911.64	-2.93	5.26E-38	DMC	26.82%	44.78%	17.96%	7.90E-06
HMPREF1322_RS00725	-	lactate utilization protein	NZ_AJZS01000011.1	13105	14472	+	14706	+	1601	Under expr.	911.64	-2.93	5.26E-38	DMC	2.91%	21.70%	18.79%	1.52E-05
HMPREF1322_RS00725	-	lactate utilization protein	NZ_AJZS01000011.1	13105	14472	+	14744	+	1639	Under expr.	911.64	-2.93	5.26E-38	DMA	2.00%	28.52%	26.52%	1.52E-06

HMPREF1322_RS00725	-	lactate utilization protein	NZ_AJZS01000011.1	13105	14472	+	15471	+	2366	Under expr.	911.64	-2.93	5.26E-38	DMA	7.97%	28.75%	20.78%	1.11E-05
HMPREF1322_RS00730	-	hypothetical protein	NZ_AJZS01000011.1	14478	15062	+	13584	+	-894	Under expr.	1091.42	-3.38	5.01E-41	DMA	2.40%	14.66%	12.25%	5.18E-07
HMPREF1322_RS00730	-	hypothetical protein	NZ_AJZS01000011.1	14478	15062	+	13730	+	-748	Under expr.	1091.42	-3.38	5.01E-41	DMC	13.59%	58.15%	44.56%	1.13E-05
HMPREF1322_RS00730	-	hypothetical protein	NZ_AJZS01000011.1	14478	15062	+	13965	+	-513	Under expr.	1091.42	-3.38	5.01E-41	DMA	3.83%	37.85%	34.02%	4.16E-06
HMPREF1322_RS00730	-	hypothetical protein	NZ_AJZS01000011.1	14478	15062	+	14019	+	-459	Under expr.	1091.42	-3.38	5.01E-41	DMA	1.48%	34.21%	32.73%	1.48E-05
HMPREF1322_RS00730	-	hypothetical protein	NZ_AJZS01000011.1	14478	15062	+	14106	+	-372	Under expr.	1091.42	-3.38	5.01E-41	DMC	16.77%	47.36%	30.59%	7.45E-07
HMPREF1322_RS00730	-	hypothetical protein	NZ_AJZS01000011.1	14478	15062	+	14200	+	-278	Under expr.	1091.42	-3.38	5.01E-41	DMA	5.92%	18.54%	12.62%	8.66E-06
HMPREF1322_RS00730	-	hypothetical protein	NZ_AJZS01000011.1	14478	15062	+	14323	+	-155	Under expr.	1091.42	-3.38	5.01E-41	DMA	2.43%	19.81%	17.38%	1.65E-05
HMPREF1322_RS00730	-	hypothetical protein	NZ_AJZS01000011.1	14478	15062	+	14324	+	-154	Under expr.	1091.42	-3.38	5.01E-41	DMA	1.76%	17.10%	15.34%	3.75E-06
HMPREF1322_RS00730	-	hypothetical protein	NZ_AJZS01000011.1	14478	15062	+	14487	+	9	Under expr.	1091.42	-3.38	5.01E-41	DMA	0.97%	19.32%	18.35%	2.62E-06
HMPREF1322_RS00730	-	hypothetical protein	NZ_AJZS01000011.1	14478	15062	+	14511	+	33	Under expr.	1091.42	-3.38	5.01E-41	DMA	4.96%	46.35%	41.39%	3.60E-06
HMPREF1322_RS00730	-	hypothetical protein	NZ_AJZS01000011.1	14478	15062	+	14512	+	34	Under expr.	1091.42	-3.38	5.01E-41	DMA	5.03%	41.65%	36.62%	1.56E-05
HMPREF1322_RS00730	-	hypothetical protein	NZ_AJZS01000011.1	14478	15062	+	14542	+	64	Under expr.	1091.42	-3.38	5.01E-41	DMC	15.67%	34.20%	18.53%	8.76E-06
HMPREF1322_RS00730	-	hypothetical protein	NZ_AJZS01000011.1	14478	15062	+	14644	+	166	Under expr.	1091.42	-3.38	5.01E-41	DMA	5.20%	29.07%	23.87%	4.28E-06
HMPREF1322_RS00730	-	hypothetical protein	NZ_AJZS01000011.1	14478	15062	+	14669	+	191	Under expr.	1091.42	-3.38	5.01E-41	DMC	7.23%	19.84%	12.61%	1.28E-05
HMPREF1322_RS00730	-	hypothetical protein	NZ_AJZS01000011.1	14478	15062	+	14693	+	215	Under expr.	1091.42	-3.38	5.01E-41	DMC	14.07%	38.73%	24.67%	1.77E-05
HMPREF1322_RS00730	-	hypothetical protein	NZ_AJZS01000011.1	14478	15062	+	14698	+	220	Under expr.	1091.42	-3.38	5.01E-41	DMC	26.82%	44.78%	17.96%	7.90E-06
HMPREF1322_RS00730	-	hypothetical protein	NZ_AJZS01000011.1	14478	15062	+	14706	+	228	Under expr.	1091.42	-3.38	5.01E-41	DMC	2.91%	21.70%	18.79%	1.52E-05
HMPREF1322_RS00730	-	hypothetical protein	NZ_AJZS01000011.1	14478	15062	+	14744	+	266	Under expr.	1091.42	-3.38	5.01E-41	DMA	2.00%	28.52%	26.52%	1.52E-06
HMPREF1322_RS00730	-	hypothetical protein	NZ_AJZS01000011.1	14478	15062	+	15471	+	993	Under expr.	1091.42	-3.38	5.01E-41	DMA	7.97%	28.75%	20.78%	1.11E-05
HMPREF1322_RS00740	-	ABC transporter ATP-binding protein	NZ_AJZS01000011.1	16133	17839	-	15471	+	-662	Under expr.	7059.72	-2.68	5.06E-10	DMA	7.97%	28.75%	20.78%	1.11E-05
HMPREF1322_RS00740	-	ABC transporter ATP-binding protein	NZ_AJZS01000011.1	16133	17839	-	17614	+	1481	Under expr.	7059.72	-2.68	5.06E-10	DMA	2.76%	16.42%	13.66%	1.15E-05
HMPREF1322_RS00740	-	ABC transporter ATP-binding protein	NZ_AJZS01000011.1	16133	17839	-	18653	+	2520	Under expr.	7059.72	-2.68	5.06E-10	DMC	4.65%	18.69%	14.04%	2.34E-05
HMPREF1322_RS00745	-	ABC transporter ATP-binding protein	NZ_AJZS01000011.1	17886	19607	-	17614	+	-272	Under expr.	3619.54	-4.27	2.40E-57	DMA	2.76%	16.42%	13.66%	1.15E-05
HMPREF1322_RS00745	-	ABC transporter ATP-binding protein	NZ_AJZS01000011.1	17886	19607	-	18653	+	767	Under expr.	3619.54	-4.27	2.40E-57	DMC	4.65%	18.69%	14.04%	2.34E-05
HMPREF1322_RS00745	-	ABC transporter ATP-binding protein	NZ_AJZS01000011.1	17886	19607	-	19392	+	1506	Under expr.	3619.54	-4.27	2.40E-57	DMA	7.54%	25.19%	17.66%	1.14E-05
HMPREF1322_RS03650	-	4-alpha-glucanotransferase	NZ_AJZS01000038.1	2961	4847	-	3558	-	597	Under expr.	5951.7	-2.22	5.69E-14	DMC	5.53%	95.22%	89.69%	4.16E-07
HMPREF1322_RS03650	-	4-alpha-glucanotransferase	NZ_AJZS01000038.1	2961	4847	-	3559	-	598	Under expr.	5951.7	-2.22	5.69E-14	DMA	4.43%	89.64%	85.21%	7.67E-08
HMPREF1322_RS03650	-	4-alpha-glucanotransferase	NZ_AJZS01000038.1	2961	4847	-	3560	-	599	Under expr.	5951.7	-2.22	5.69E-14	DMA	1.45%	86.22%	84.77%	5.31E-06
HMPREF1322_RS06180	-	Ppx/GppA family phosphatase	NZ_AJZS01000066.1	22201	23108	-	22242	-	41	Over expr.	914.83	1.59	2.19E-12	DMA	15.95%	96.80%	80.86%	3.66E-07

HMPREF1322_RS06180	-	Ppx/GppA family phosphatase	NZ_AJZS01000066.1	22201	23108	-	22243	-	42	Over expr.	914.83	1.59	2.19E-12	DMC	10.21%	64.13%	53.91%	6.11E-07
HMPREF1322_RS06180	-	Ppx/GppA family phosphatase	NZ_AJZS01000066.1	22201	23108	-	22938	-	737	Over expr.	914.83	1.59	2.19E-12	DMA	85.99%	37.41%	48.59%	4.56E-06
HMPREF1322_RS06180	-	Ppx/GppA family phosphatase	NZ_AJZS01000066.1	22201	23108	-	22943	+	742	Over expr.	914.83	1.59	2.19E-12	DMC	70.43%	31.90%	38.53%	2.21E-05

Strand Expr: Strand of the gene
Strand Meth: Strand of the methylated position
Distance Meth: Distance of the methylated position to the gene start site in base pairs, negative values indicate upstream location
DE analysis: results from the differential expression analysis
DM analysis: results from the differential methylation analysis
LFC: log_2 fold change
LiH: growth in limited hemin
ExH: growth in excess hemin